THE GEOLOGICAL SOCIETY OF AMERICA®

Neoarchean large igneous provinces on the Kaapvaal Craton in southern Africa re-define the formation of the Ventersdorp Supergroup and its temporal equivalents

Ashley Gumsley[1,2,†], Joaen Stamsnijder[1], Emilie Larsson[1], Ulf Söderlund[1,3], Tomas Naeraa[1], Michiel de Kock[4], Anna Sałacińska[5], Aleksandra Gawęda[6], Fabien Humbert[4], and Richard Ernst[7,8]

[1]*Department of Geology, Lund University, Lund, Sweden*
[2]*Institute of Geophysics, Polish Academy of Sciences, Warsaw, Poland*
[3]*Department of Geosciences, Swedish Museum of Natural History, Stockholm, Sweden*
[4]*Department of Geology, University of Johannesburg, Johannesburg, South Africa*
[5]*Institute of Geological Sciences, Polish Academy of Sciences, Warsaw, Poland*
[6]*Institute of Earth Sciences, University of Silesia in Katowice, Sosnowiec, Poland*
[7]*Department of Earth Sciences, Carleton University, Ottawa, Canada*
[8]*Faculty of Geology and Geography, Tomsk State University, Tomsk, Russia*

ABSTRACT

U-Pb geochronology on baddeleyite is a powerful technique that can be applied effectively to chronostratigraphy. In southern Africa, the Kaapvaal Craton hosts a well-preserved Mesoarchean to Paleoproterozoic geological record, including the Neoarchean Ventersdorp Supergroup. It overlies the Witwatersrand Supergroup and its world-class gold deposits. The Ventersdorp Supergroup comprises the Klipriviersberg Group, Platberg Group, and Pniel Group. However, the exact timing of formation of the Ventersdorp Supergroup is controversial. Here we present 2789 ± 4 Ma and 2787 ± 2 Ma U-Pb isotope dilution-thermal ionization mass spectrometry (ID-TIMS) baddeleyite ages and geochemistry on mafic sills intruding the Witwatersrand Supergroup, and we interpret these sills as feeders to the overlying Klipriviersberg Group flood basalts. This constrains the age of the Witwatersrand Supergroup and gold mineralization to at least ca. 2.79 Ga. We also report 2729 ± 5 Ma and 2724 ± 7 Ma U-Pb ID-TIMS baddeleyite ages and geochemistry from a mafic sill intruding the Pongola Supergroup and on an east-northeast–trending mafic dike, respectively. These new ages distinguish two of the Ventersdorp Supergroup magmatic events: the Klipriviersberg and Platberg. The Ventersdorp Supergroup can now be shown to initiate and terminate with two large igneous provinces (LIPs), the Klipriviersberg and Allanridge, which are separated by Platberg volcanism and sedimentation. The age of the Klipriviersberg LIP is 2791–2779 Ma, and Platberg volcanism occurred at 2754–2709 Ma. The Allanridge LIP occurred between 2709–2683 Ma. Klipriviersberg, Platberg, and Allanridge magmatism may be genetically related to mantle plume(s). Higher heat flow and crustal melting resulted as a mantle plume impinged below the Kaapvaal Craton lithosphere, and this was associated with rifting and the formation of LIPs.

INTRODUCTION

Major intraplate magmatic events, many of which generate large igneous provinces (LIPs), are globally becoming better understood through U-Pb dating of their magmatic feeders: mafic dike swarms and sill provinces. Although the definition of LIPs has become increasingly complex, a LIP is typically defined as a mainly mafic magmatic province that is >0.1 Mkm^2 in area, with volumes >0.1 Mkm^3 (Ernst, 2014). Usually, LIPs are emplaced within 1–5 m.y. or consist of multiple short pulses over a maximum of a few tens of millions of years (Ernst and Youbi, 2017) and geochemically have intraplate characteristics. Additionally, many mafic dike swarms and sill provinces connected with LIPs intrude supracrustal successions and can be crucial temporal markers in the stratigraphic record or help to constrain the timing of critical events in the Earth's history (e.g., Ernst and Youbi, 2017; Gumsley et al., 2017).

The Ventersdorp Supergroup (Fig. 1) on the Kaapvaal Craton in southern Africa is the largest and oldest predominantly volcanic supracrustal succession in the world and has been linked to the slightly lower volume Fortescue Group on the Pilbara Craton; both may have been contiguous in the hypothetical Vaalbara Supercraton (de Kock et al., 2009; Evans et al., 2017). The Ventersdorp Supergroup overlies the world-class gold- and uranium-bearing conglomerate reefs of the Witwatersrand Supergroup. However, the exact timing of the formation of the Ventersdorp Supergroup has been a matter of controversy, with implications for the termination of Witwatersrand Supergroup and gold deposition (Armstrong et al., 1991; Wingate, 1998; de Kock et al., 2012; Cornell et al., 2017). Armstrong et al. (1991) reported 2714 ± 16 Ma and 2709 ± 8 Ma ages (Table 1) for the lower (Klipriviersberg Group) and middle (Makwassie Formation of the Platberg Group) part of the Ventersdorp Supergroup, respectively, making the whole volcanic province a single, but pulsed LIP, ~10 m.y. long, connected with a mantle plume (e.g., Eriksson et al., 2002). However, several authors have argued for a longer and older period of formation between ca. 2.78 Ga and ca. 2.71 Ga (Wingate, 1998; de Kock et al., 2012; Cornell et al., 2017). For example, Cornell et al. (2017) re-dated the quartz porphyry of the Makwassie Formation at 2720 ± 2 Ma (Table 1), calling into question the age of ca. 2709 Ma obtained by Armstrong et al. (1991) for the same unit, as well as the ca. 2714 Ma age for underlying flood basalts of the Klipriviersberg Group. Similarly contradicting ages (i.e., older than ca.

†agumsley@igf.edu.pl.

 https://doi.org/10.1130/B35237.1; 9 figures; 1 table; Data Repository item 2020050.

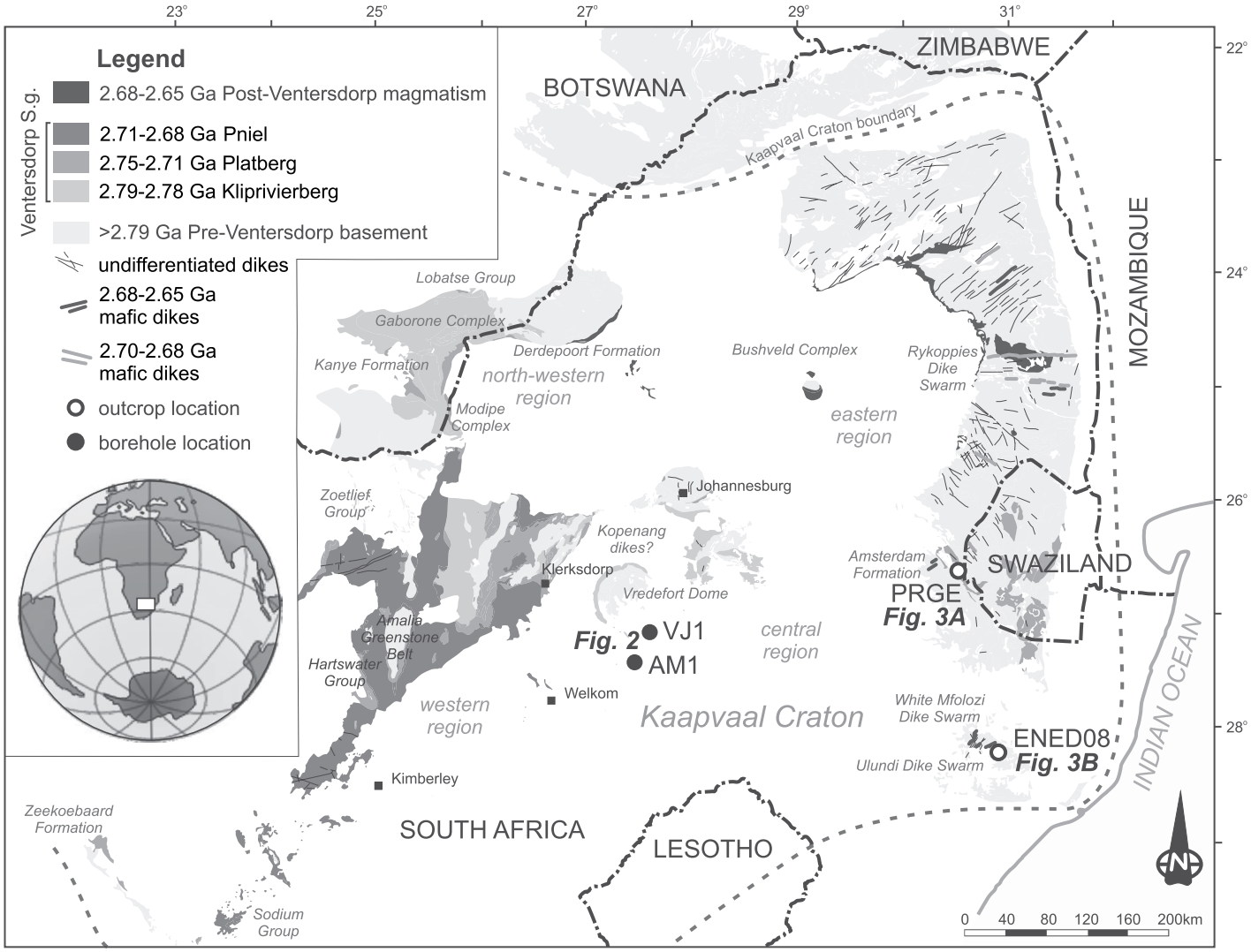

Figure 1. Geological map of eastern southern Africa (including sample localities) showing units of interest in this study formed between ca. 2.8 Ga and ca. 2.6 Ga. The map includes the Ventersdorp Supergroup and its temporally equivalent units overlying the older Archean basement. Maps modified after Wiles (1971), Jones and Hepworth (1973), and Keyser (1997). Bold mafic dikes are dated and define their respective dike swarms. Sampling areas are indicated in the central and southeastern regions of the Kaapvaal Craton.

2714 Ma) were determined from units that are lithostratigraphically similar to the Ventersdorp Supergroup from the northwestern and western regions of the Kaapvaal Craton (Table 1; e.g., Wingate, 1998; de Kock et al., 2012). The exact correlation of these units to the Ventersdorp Supergroup, however, has yet to be confirmed. It has also been argued that Ventersdorp Supergroup magmatism represent three pulses, or potentially three different LIP events (Ernst and Buchan, 2001; Ernst, 2014).

In this study, mafic sills and dikes intruding units older than the Ventersdorp Supergroup (i.e., the Witwatersrand Supergroup, the Pongola Supergroup, and the basement granitoids and granitic gneisses of the Kaapvaal Craton) provide new chronostratigraphic information for the Ventersdorp Supergroup. This information further constrains the timing and formation of the Ventersdorp Supergroup and temporally related units. For the first time, in conjunction with previous studies, we can now define LIPs as initiating, developing, and terminating the formation of the Ventersdorp Supergroup over a period of ~100 m.y. (e.g., Ernst and Buchan, 2001). The Witwatersrand Supergroup and its world-class gold deposits can also now be shown to have formed by ca. 2.79 Ga.

REGIONAL GEOLOGY

The Kaapvaal Craton in southern Africa preserves over ca. 3.6 Ga of geological history and is world renowned for its record of well-preserved Archean rocks. Following the stabilization of the proto-craton around ca. 3.1 Ga, a series of five supracrustal successions developed unconformably on a peneplaned basement terrain of greenstone belts and greenstone fragments, granitic gneisses, and granitoid plutons before the intrusion of the Bushveld Complex between 2056 Ma and 2055 Ma (Zeh et al., 2015). These five supracrustal successions, in chronological order, include the Dominion Group, Pongola Supergroup, Witwatersrand Supergroup, Ventersdorp Supergroup, and Transvaal Supergroup. The Mesoarchean Dominion Group and the Witwatersrand Supergroup can be regarded as stratigraphic equivalents of the Pongola Supergroup (Beukes and Cairncross, 1991; Cole, 1994).

TABLE 1. COMPILATION OF CRYSTALLIZATION AGES OF ROCKS OBTAINED BY U-Pb GEOCHRONOLOGY OF ZIRCON AND BADDELEYITE. SOURCES IN SUPPLEMENTARY INFORMATION

	Unit	Region	Rock type	Age	±2σ	Mineral	Source
1	Lovedale	W	kimberlite	2630	1	zircon	1
2	Vryburg	W	lava	2642	4	zircon	2
3	Vryburg	W	tuff	2642	6	zircon	2
4	Pre-Morokweng	W	granophyre	2689	10	zircon	3
5	Kareefontein	W	quartz porphyry	2714	6	zircon	4
6	Zoetlief	W	lava	2717	6	zircon	2
7	Skalkseput	W	granite	2718	16	zircon	5
8	Kareefontein	W	dacite	2718	6	zircon	6
9	Steenkop	W	granite	2719	12	zircon	7
10	Skalkseput	W	monzogranite dike	2720	9	zircon	7
11	Steenkop	W	monzogranite	2722	14	zircon	7
12	Makwassie	W	rhyolite	2723	6	zircon	6
13	Hartswater	W	quartz-feldspar porphyry	2724	6	zircon	8
14	Paardefontein	W	rhyolite	2729	3	zircon	9
15	Hartswater	W	tuff	2733	3	zircon	8
16	Ongers River	W	rhyolite	2739	10	zircon	10
17	Mosita	W	granite	2749	4	zircon	11
18	Amalia	W	tuff	2754	10	zircon	2
19	Goedgenoeg	W	dacite	2781	5	zircon	6
20	Mosita	W	adamellite	2791	8	zircon	12
21	Buffelsfontein	NW	lava	2658	16	zircon	2
22	Buffelsfontein	NW	felsite	2664	1	zircon	13
23	Derdepoort	NW	basalt	2769	2	zircon	14
24	Kgale	NW	granite	2779	6	zircon	15
25	Derderpoort	NW	felsite	2781	10	zircon	16
26	Kgale	NW	granite	2782	10	zircon	15
27	Plantation	NW	porphyry	2782	4	zircon	17
28	Kgale	NW	granite	2783	4	zircon	15
29	Modipe	NW	gabbro	2784	1	baddeleyite	18
30	Kanye	NW	volcanic	2784	8	zircon	15
31	Kanye	NW	rhyolite	2785	4	zircon	19
32	Kanye	NW	lava	2785	4	zircon	19
33	Ntantlhe	NW	granophyre	2785	4	zircon	19
34	Vereeniging	C	gabbroid	2629	6	zircon	2
35	Makwassie	C	quartz porphyry	2709	8	zircon	20
36	Klipriviersberg	C	quartz porphyry	2714	16	zircon	20
37	Makwassie	C	rhyolite	2721	6	zircon	6
38	Makwassie	C	rhyolite	2722	6	zircon	6
39	Welkom West	C	granitoid	2727	12	zircon	21
40	Goedgenoeg	C	dacite	2746	9	zircon	6
41	**Witwatersrand**	**C**	**sill (AM1)**	**2787**	**2**	**baddeleyite**	**this study**
42	**Witwatersrand**	**C**	**sill (VJ1)**	**2789**	**4**	**baddeleyite**	**this study**
43	Mantenga	E	pegmatite	2652	6	zircon	2
44	White Mfolozi dike swarm	E	dike	2654	2	baddeleyite	22
45	White Mfolozi dike swarm	E	dike	2659	5	baddeleyite	22
46	White Mfolozi dike swarm	E	dike	2659	1	baddeleyite	22
47	Rykoppies dike swarm	E	dike	2659	20	baddeleyite	23
48	White Mfolozi dike swarm	E	dike	2661	13	baddeleyite	22
49	White Mfolozi dike swarm	E	dike	2661	4	baddeleyite	22
50	White Mfolozi dike swarm	E	dike	2662	3	baddeleyite	22
51	Rykoppies dike swarm	E	dike	2662	8	baddeleyite	23
52	White Mfolozi dike swarm	E	dike	2664	4	baddeleyite	22
53	Kwetta	E	granite	2671	6	zircon	unpublished
54	Rykoppies dike swarm	E	dike	2683	7	baddeleyite	23
55	Mbabane	E	granitoid	2691	8	zircon	24
56	Rykoppies dike swarm	E	dike	2692	7	baddeleyite	25
57	Rykoppies dike swarm	E	dike	2698	10	baddeleyite	23
58	Rykoppies dike swarm	E	dike	2701	19	baddeleyite	25
59	Spekboom	E	granite	2714	19	zircon	26
60	Mswati	E	granitoid	2717	11	zircon	27
61	Ngwempisi	E	granite	2720	8	zircon	2
62	Kwetta	E	granite	2720	10	zircon	27
63	Kwetta	E	granite	2721	16	zircon	27
64	Hlatikulu	E	granite	2722	14	zircon	28
65	Kwetta	E	granite	2722	12	zircon	2
66	Sicunusu	E	granite	2723	14	zircon	2
67	**Witwatersrand**	**E**	**sill (PRGE)**	**2727**	**3**	**baddeleyite**	**this study**
68	Usutu	E	granite	2729	1	zircon	29
69	**Pongola**	**E**	**dike (ENED08)**	**2729**	**5**	**baddeleyite**	**this study**
70	Usutu	E	granite	2730	0	zircon	29
71	Nzimane	E	granite	2733	6	zircon	2
72	Mpageni	E	granite	2740	15	zircon	30

Notes: Regions: E—east; C—central; W—west; NW—northwest. Data were filtered assuming <20 Ma ± 2σ. Numbers in source refer to the references in Table DR9.

The ~300,000 km^2 Neoarchean Ventersdorp Supergroup (e.g., van der Westhuizen et al., 1991, 2006) is a supracrustal volcanic-sedimentary succession (Fig. 1). The development of the Ventersdorp Supergroup has been attributed to a mantle plume arising from the core-mantle boundary, which led to the formation of a LIP that was distinctly pulsed (Hatton, 1995; Ernst, 2014). In Olsson et al. (2011), a mantle plume center for the Ventersdorp LIP was proposed beneath the Bushveld Complex. The Ventersdorp Supergroup comprises the basal Klipriviersberg Group, followed by the Platberg Group, the Bothaville Formation, and finally the Allanridge Formation. The last two formations comprise the Pniel Group (South African Committee for Stratigraphy (SACS), 1980). At its base, the Ventersdorp Supergroup is separated from the Witwatersrand Supergroup by an unconformity in the central part of the Kaapvaal Craton (e.g., van der Westhuizen et al., 2006). However, in isolated parts of the center of the basin, a conformable relationship exists where conglomerates of the Venterspost Formation (also known

as the Ventersdorp contact reef or VCR) are sporadically developed (e.g., Pelletier, 1937; Chunnett, 1994). This formation gives way to the ca. 2714 Ma Klipriviersberg Group flood basalts (Winter, 1976; Armstrong et al., 1991). In the North West Province of South Africa, and southwestern Botswana (Fig. 1), a lithostratigraphically similar succession of flood basalts within the Derdepoort Formation was correlated to the Klipriviersberg Group (e.g., Tyler, 1979). The Derdepoort Formation, however, was inferred by Wingate (1998) at 2782 ± 5 Ma, leading him to regard the 2714 ± 16 Ma age of Armstrong et al. (1991) as a minimum age for Klipriviersberg Group volcanism. The Derdepoort Formation is also coeval to nearby bimodal volcanic rocks and plutonic units in southwestern Botswana and the North West Province of South Africa. In this area (Fig. 1), the Lobatse Group and Kanye Formation have also been dated between ca. 2785 Ma and ca. 2781 Ma (Table 1; Grobler and Walraven, 1993; Moore et al., 1993; Walraven et al., 1996), while the Modipe Complex gabbro and Gabarone Complex granite (Fig. 1) have yielded ages between 2784 Ma and 2779 Ma, respectively (Grobler and Walraven, 1993; Moore et al., 1993; Mapeo et al., 2004; Denyszyn et al., 2013). The only indication that this dated series of coeval magmatic events may have been spatially more significant is an age of 2781 ± 5 Ma for a dacite in a drill core ~480 km to the southwest, near Kimberley (Fig. 1; Cornell et al., 2017). It has thus been speculated that the Klipriviersberg Group forms part of this ca. 2.78 Ga magmatic pulse (Wingate, 1998; de Kock et al., 2012), but prior to this study, such ages were not reported from the central region of the Kaapvaal Craton, which is the type area of the Klipriviersberg Group.

An unconformity separates the Klipriviersberg Group from the Platberg Group (van der Westhuizen et al., 2006); the Platberg Group formed within numerous grabens and half grabens following the termination of Klipriviersberg Group volcanism (Winter, 1976; Stanistreet and McCarthy, 1991). The Platberg Group is best developed over the western Witwatersrand Supergroup in the central part of the Kaapvaal Craton and farther westward (Fig. 1; e.g., Tankard et al., 1982). The typical Platberg Group graben-fill succession consists of basal, coarse-grained sedimentary rocks of the Kameeldoorns Formation, followed by predominantly more mafic volcanic rocks of the Goedgenoeg Formation and more felsic volcanic rocks of the Makwassie Formation (Winter, 1976; Armstrong et al., 1991; van der Westhuizen et al., 2006). In some instances, interbedded mafic volcanic and sedimentary rock (i.e., the Rietgat Formation) is developed overlying the typical successions, but its occurrence is limited to reactivated grabens (van der Westhuizen et al., 2006). Graben-fill is characterized by rapid facies changes and wedge-shaped geometries (de Kock et al., 2012), with possible caldera formation accounting for the excessively thick formations (Meintjes and van der Westhuizen, 2018a). The Makwassie Formation has been dated by Armstrong et al. (1991) at 2709 ± 8 Ma and more recently by Cornell et al. (2017) at 2720 ± 2 Ma at several localities (Table 1). Cornell et al. (2017) further presented an age for the underlying Goedgenoeg Formation of 2746 ± 9 Ma (Table 1). These ages by Cornell et al. (2017) for the Platberg Group are in agreement with age constraints from many lithological correlatives of the Ventersdorp Supergroup that have been described under various names due to non-continuous outcrop in isolated grabens (Fig. 1; van der Westhuizen et al., 2006). These include the 2739 ± 10 Ma Sodium Group (Altermann and Lenhardt, 2012), the 2714 ± 3 Ma Zoetlief Group (Walraven et al., 1991), the 2729 ± 3 Ma Amalia Group (Poujol et al., 2005), and the 2733–2724 Ma Hartswater Group (de Kock et al., 2012) (see Table 1). It has been suggested that the age differences between Platberg Group equivalents is a result of diachronous graben development across the Kaapvaal Craton (de Kock et al., 2012). All these U-Pb ages are in disagreement with the younger ca. 2714 Ma age for the Klipriviersberg Group, which is stratigraphically beneath the Platberg Group.

The so-called Pniel Group overlies the Platberg Group with an unconformity (Winter, 1976) that followed the cessation of graben development (Stanistreet and McCarthy, 1991). The Pniel Group covers an extensive area in the central and western parts of the Kaapvaal Craton (van der Westhuizen et al., 2006). The base of the Pniel Group, the Bothaville Formation, is composed of an upward-fining succession of conglomerates and sandstones (Visser and Grobler, 1985). The basaltic andesites of the Allanridge Formation (Winter, 1976) are conformable with the underlying Bothaville Formation (van der Westhuizen et al., 2006). The Pniel Group has not been dated directly, but a maximum age constraint of 2720 ± 4 Ma is available for the lithostratigraphically equivalent Zeekoebaart Formation of the southwestern margin of the Kaapvaal Craton (Fig. 1 and Table 1; Cornell et al., 2018). A minimum age constraint comes from a 2664 ± 1 Ma age for volcanic rocks at the base of the overlying Transvaal Supergroup in the Buffelsfontein Group (Table 1; Barton et al., 1995). The Allanridge Formation is ascribed to renewed rifting and thermal subsidence of the Kaapvaal Craton after the cessation of volcanism in the Platberg Group (Burke et al., 1985; Clendenin et al., 1988).

Mafic dike emplacement on the stabilized Kaapvaal Craton is summarized in de Kock et al. (2019), and the first known dike swarm occurred between ca. 2980 Ma and ca. 2966 Ma, with the southeast–trending Badplaas Dike Swarm on the southeastern region of the Kaapvaal Craton (Olsson et al., 2010; Gumsley et al., 2015). These dikes are temporally and spatially associated with the Nsuze Group of the Pongola Supergroup and the Piet Retief Suite of the Usushwana Complex (Olsson et al., 2010; Gumsley et al., 2015). Further mafic magmatism was manifest later in a mafic sill province hosted within the Pongola Supergroup, which includes the 2866 ± 2 Ma Hlagothi Complex (Gumsley et al., 2013; 2015). The Modipe Complex was then emplaced at 2784 ± 1 Ma (Fig. 1 and Table 1; Denyszyn et al., 2013), which is temporally associated with the Gabarone Complex granite and volcanism within the nearby Derdepoort and Kanye Formations (Grobler and Walraven, 1993; Moore et al., 1993; Walraven et al., 1996; Wingate, 1998; Mapeo et al., 2004) on the northwestern region of the Kaapvaal Craton. Approximately 80 m.y. later, mafic magmatism was again documented between ca. 2701 Ma and ca. 2654 Ma on the eastern and southeastern regions of the Kaapvaal Craton (Fig. 1 and Table 1; Olsson et al., 2010, 2011; Gumsley et al., 2016). This includes the 2701 ± 11 Ma to 2659 ± 13 Ma Rykoppies Dike Swarm, which appears to radiate out from beneath the 2056–2055 Ma Bushveld Complex (Olsson et al., 2011; Zeh et al., 2015) and the 2664–2654 Ma northeast–trending White Mfolozi Dike Swarm (Table 1; Gumsley et al., 2016). The Rykoppies and White Mfolozi Dike Swarms potentially mark the termination of Ventersdorp Supergroup-related magmatism at ca. 2.65 Ga, as these dike swarms are also coeval with 2664 ± 1 Ma proto-basinal volcanism to the Transvaal Supergroup in the Buffelsfontein Group (Barton et al., 1995), as well as other proto-basins. Lastly, there are the so-called Kopenang dikes, which were documented by Meier et al. (2009) on the central region of the Kaapvaal Craton within the Witwatersrand Supergroup, although they have random trends. Meier et al. (2009) linked these mafic dikes geochemically to the Klipriviersberg Group. However, their exact relationship remains to be confirmed.

SAMPLING

In this study, three samples of mafic sills and one sample from a mafic dike are examined (Table DR1[1]). Two samples, named AM1 and VJ1, were collected from drillcore near one of

[1]GSA Data Repository item 2020050, supplementary data tables DR1–DR10, is available at http://www.geosociety.org/datarepository/2020 or by request to editing@geosociety.org.

the type areas of the Ventersdorp Supergroup in the central region of the Kaapvaal Craton in the Free State Province of South Africa (Fig. 1). Another two samples, PRGE and ENED08, were collected from outcrops in the southeastern (Mpumalanga Province) and southeasternmost (KwaZulu-Natal Province) regions of the Kaapvaal Craton in South Africa (Fig. 1).

Mafic intrusive rocks are commonly intersected in boreholes through Precambrian strata and especially within the Witwatersrand Supergroup on the central region of the Kaapvaal Craton. Many are sills that are over ~100 m thick, including the studied sills, which are stratigraphically below the flood basalts of the Klipriviersberg Group. The sills are weakly metamorphosed and deformed along with the Witwatersrand Supergroup strata they intruded. The AM1 and VJ1 mafic sills are located east of Klerksdorp and Welkom but south of the Vredefort Dome. The sills intruded into the Government Subgroup of the upper West Rand Group from the Witwatersrand Supergroup (Fig. 2). Sample VJ1 was collected from drill core ~10 km northeast of Edenville from a ~200-m-thick mafic sill at ~1400 m depth, which intruded into sandstones of the Palmietfontein Formation. Sample AM1 was collected from a drill core ~10 km north of Steynsrus (Fig. 2) and comes from a ~110-m-thick mafic sill at ~1800 m depth that intruded into sandstones of the Afrikaner Formation.

Another mafic sill, PRGE, was sampled near the road between Piet Retief and Amsterdam in southeast Mpumalanga (Fig. 3A). The outcrop is on the border between the Evergreen and Redcliff Farms, with the mafic sill intruding into the Redcliff Formation. The Redcliff Formation, comprising shales and banded iron formation, and has been assigned to the Mozaan Group of the Pongola Supergroup. The mafic sill itself was previously ascribed to the 2990–2978 Ma Piet Retief Suite of the Usushwana Complex (Hammerbeck, 1982; Gumsley et al., 2015).

Sample ENED-08 is from an east-northeast–trending mafic dike that was sampled near the White Mfolozi River between Ulundi and Vryheid (Fig. 3B). The dike intrudes the 3254–3234 Ma granitoid gneiss basement in the White Mfolozi inlier of northern KwaZulu-Natal (Reinhardt et al., 2015) and is part of a mafic dike swarm, herein termed the Ulundi Dike Swarm. This dike swarm is in turn cut by the 2664–2654 Ma plagioclase–megacrystic, northeast–trending White Mfolozi Dike Swarm (Gumsley et al., 2016). Further, the sampled dike cuts an undated southeast–trending mafic dike; both are in turn cut by a ca. 2423 Ma mafic sheet (Gumsley et al., 2017). Some geochemistry and paleomagnetism on these mafic units was conducted by Klausen et al. (2010) and Lubnina et al. (2010).

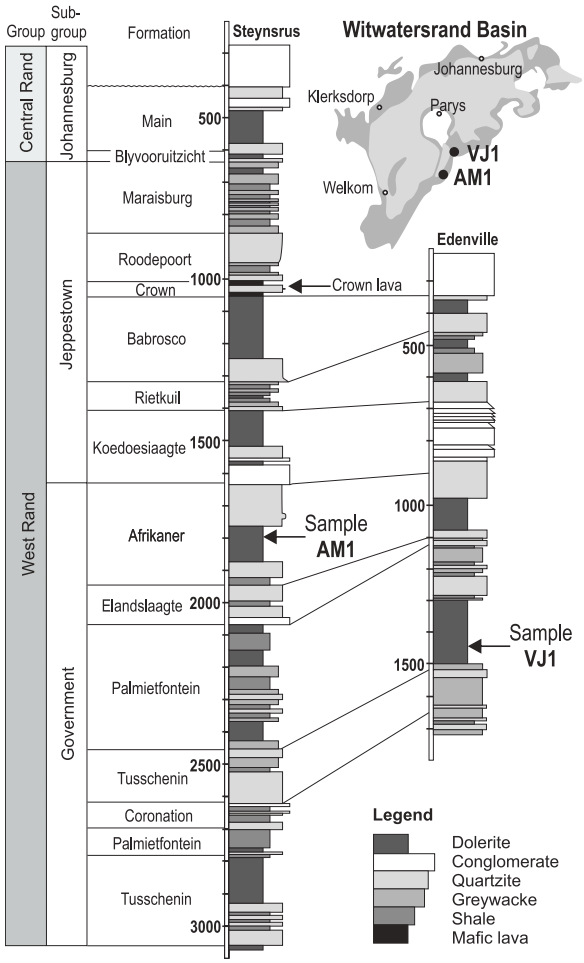

Figure 2. Locality map and stratigraphic log of boreholes from which mafic sill sample AM1 and VJ1 were collected in the Witwatersrand Supergroup on the central region of the Kaapvaal Craton, between Steynsrus and Edenville, respectively.

METHODOLOGY

Petrography

Petrographic analysis of thin sections was undertaken at the Institute of Earth Sciences in the University of Silesia in Katowice using an Olympus BX-51 optical microscope. Mineral chemical analysis of the main rock-forming and accessory minerals was carried out at the Inter-Institutional Laboratory of Microanalyses of Minerals and Synthetic Substances, University of Warsaw, using a CAMECA SX-100 electron microprobe. The analytical conditions employed an accelerating voltage of 15 kV, a beam current of 20 nA, counting times of 4 s for the peaks and

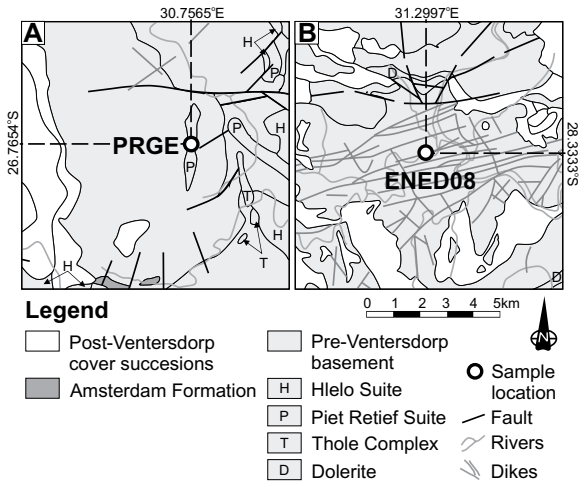

Figure 3. Geological map of sample localities for (A) mafic sill PRGE near Amsterdam and (B) east-northeast–trending mafic dike ENED08 from the Ulundi Dike Swarm on the White Mfolozi River near Ulundi, both on the southeastern region of the Kaapvaal Craton. GPS coordinates are shown. Maps modified after Walraven (1986) and Coetzee (1988).

background, and a beam diameter of 1–5 µm. Reference materials, analytical lines, and mean detection limits (in wt. %) can be found in Table DR2 (see footnote 1). Diffracting crystals include LIF, PET, TAP, and LPET.

Whole-Rock Major and Trace Element Geochemistry

For whole-rock geochemistry, samples were selected from the most homogenous parts of the sampled mafic sills and dike after the weathered material was removed. They were then hand crushed and milled in a tungsten-carbide ring mill. The resulting material was then coned and quartered before being dispatched for analysis of major, minor, and trace elements at Bureau Veritas Laboratories in Vancouver, Canada. Analyses were made on glass beads prepared from the powdered samples with a sample-to-flux (lithium tetraborate) ratio of 1:10, and the resulting molten bead was rapidly digested in weak nitric acid solution. Inductively coupled plasma emission spectroscopy (ICPES) was used for major and minor elements, and inductively coupled plasma mass spectrometry (ICPMS) was used for trace elements, including rare-earth elements (REE). The volatile content of each sample was determined by loss on ignition (LOI). The data were plotted in diagrams using the GeoChemical Data toolkit (GCDkit; Janoušek et al., 2006).

U-Pb Baddeleyite Geochronology

The sampled units were processed for baddeleyite U-Pb dating by the isotope dilution-thermal ionization mass spectrometry (ID–TIMS) and laser ablation (LA)–ICPMS analytical methodologies. The LA–ICPMS methodology was deployed to test the reproducibility between the two independent methods at the LA–ICPMS Laboratory at Lund University. Samples were hand crushed and ground to a coarse-grained powder using a chrome-steel ring mill in the Department of Geology, Lund University. The water-based separation process developed by Söderlund and Johansson (2002) was used to extract baddeleyite grains for ID-TIMS; however, only VJ1 yielded suitably sized baddeleyite grains for LA-ICPMS (greater than 60 µm long and 20 µm wide).

ID-TIMS

The extracted baddeleyite grains were split into fractions that were transferred in ethanol to pre-cleaned Teflon capsules. The fractions were washed for several cycles in ultrapure HNO_3 and H_2O. A small amount of a $^{236–233}U$-^{205}Pb tracer solution and an ultrapure HF:HNO_3 (10:1) mixture was added to each Teflon capsule. The baddeleyite fractions were completely dissolved in an oven after three days at ~190 °C. The capsules were placed on a hotplate at ~100 °C until the HF solution had evaporated. A mixture of ultrapure 0.25 M H_3PO_4 and 6.2 M HCl was added to each capsule and dried again on a hotplate. The remaining sample droplet in the Teflon capsules was mixed with 2 µl of a prepared Si gel and placed on an outgassed Re filament. The samples on the outgassed Re filaments were heated until the H_3PO_4 burnt off. The resultant filaments were then placed in a carousel inside a Finnigan TRITON thermal ionization mass spectrometer at the Department of Geosciences, Swedish Museum of National History in Stockholm. The mass spectrometer is equipped with a secondary electron multiplier and Faraday Cups.

The Re filaments and samples were heated to temperatures between ~1210 °C and ~1250 °C, where the intensities of the isotopic masses of ^{204}Pb, ^{205}Pb, ^{206}Pb, ^{207}Pb, and ^{208}Pb were measured in cycles of between 20 and 140 at gradually increasing temperatures. The Pb signal intensities were measured in either static mode with Faraday Cups or in dynamic mode with peak-switching using the secondary electron multipliers. The isotopic masses of ^{233}U, ^{236}U, and ^{238}U were measured as oxides at temperatures of ~1300 °C to ~1340 °C at increasing temperatures. The ^{235}U was calculated from ^{238}U, using $^{238}U/^{235}U = 137.818$, following Hiess et al. (2012). No significant differences due to interferences from ^{18}O were detected, and therefore corrections were not made. The measurements were made in dynamic mode for between 40 and 80 cycles. Initial data reduction was made using an "in-house" Microsoft Excel program using algorithms from Ludwig (2003). However, the Microsoft Excel macro, Isoplot 4.15, from Ludwig (2012) using U decay constants from Jaffey et al. (1971), was used for final data calculations and concordia diagrams. Initial common Pb corrections were made using the isotopic compositions from the global common Pb evolution model of Stacey and Kramers (1975) at the age of the sample. Error propagations in dates are given at 2σ and do not include decay constant errors.

LA-ICPMS

Baddeleyite grains from sample VJ1 were placed on double-sided adhesive tape and mounted into epoxy resin in a 1-inch-wide Teflon ring and left to harden for three days. The hardened epoxy mount was then separated from the tape and polished for between 20 s and 140 s, with 9 µm, 3 µ, and 1 µm diamond paste using a Struers Rotopol-22 automated polisher. The mount was subsequently cleaned with ethanol. The reference material used was baddeleyite from the Phalaborwa Complex, which was dated to 2059.60 ± 0.35 Ma (Heaman, 2009).

The analyses were carried out at the LA-ICPMS Laboratory in the Department of Geology at Lund University. The LA-ICPMS uses a 193 nm Analyte G2 laser ablation unit with a two volume HelEx sample holder and an Aurora Elite quadrupole inductively coupled plasma mass spectrometer. Ablation was done with a 5 Hz repetition rate, a fluence of ~4 j/cm^2, using 20 µm spot diameters. The total acquisition time for each analysis was 55 s, of which the first 20 s were used to determine the Ar/He/N_2 gas blank, followed by 28 s of laser ablation and 3–4 s of wash-out delay. The He carrier gas was mixed downstream with Ar and N_2 before entering a "squid" signal smoothing device made up of several tubes that split the stream and re-joined it before entering the plasma. The mass spectrometer was calibrated using NIST612 glass to give stable ^{206}Pb, ^{207}Pb, and ^{238}U signals and low oxide production rates ($^{238}U^{16}O/^{238}U$ below 0.5%) and a $^{232}Th/^{238}U$ ratio of ~1. The ^{202}Hg, $^{204}(Pb + Hg)$, ^{206}Pb, ^{207}Pb, ^{208}Pb, ^{232}Th, ^{235}U, and ^{238}U intensities were determined using secondary electron multipliers. The interference of ^{204}Hg on ^{204}Pb was monitored by measuring ^{202}Hg, assuming a $^{202}Hg/^{204}Hg$ ratio of 4.36 (natural abundance). Although ^{235}U was measured, the $^{207}Pb/^{235}U$ was calculated from ^{238}U, using $^{238}U/^{235}U = 137.818$ following Hiess et al. (2012). The laser-induced elemental fractionation and instrumental mass bias on measured isotopic ratios were corrected through standard-sample bracketing using the Phalaborwa baddeleyite standard (Heaman 2009). A total of 36 analyses were made in the following order: six standards followed by seven unknowns (i.e., VJ1), four standards, six unknowns, four standards, five unknowns, and four standards. Data reduction was done using the Iolite software (Paton et al., 2011) with the U-Pb geochronology data reduction scheme routine of Paton et al. (2010). Correction routines for downhole fractionation and instrumental drift were applied in the Iolite software. Common-Pb correction was done in the Iolite software using VizaulAge by Petrus and Kamber (2012) from the terrestrial Pb-isotope composition of Stacey and Kramers (1975). All age data were calculated using Isoplot 4.15 (Ludwig, 2012), which was also used to plot and evaluate data. Error propagation in dates reported are given at 2σ and do not include decay constant errors.

RESULTS

Petrography

The four samples investigated have a mineral assemblage typical of mafic intrusions (Table

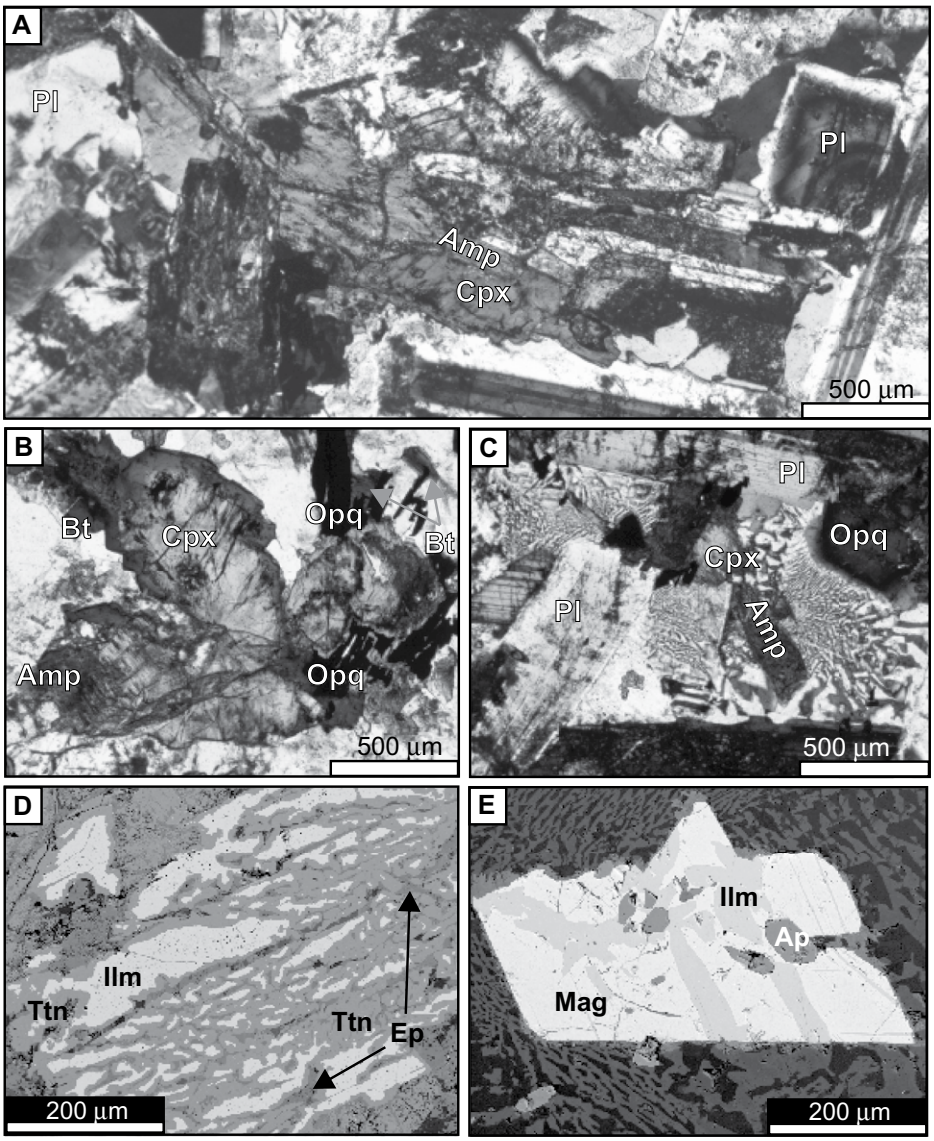

Figure 4. (A) Photomicrograph illustrating relationships of the main rock-forming minerals in the mafic sill (sample PRGE). Note the overgrowths of amphibole (Amp) on a primary clinopyroxene (Cpx) and zoned, twinned plagioclase feldspar (Pl). (B) Photomicrograph showing the overgrowths of secondary amphibole (Amp) on clinopyroxene (Cpx) and secondary biotite (Bt) on opaque minerals (Opq). (C) Photomicrograph illustrating the relationships of the groundmass formed by graphic intergrowths of quartz and alkali–feldspar with plagioclase feldspar (Pl), clinopyroxene (Cpx), and opaque phases (Opq). (D) Backscattered electron (BSE) image of an ilmenite (Ilm) replaced by titanite (Ttn). (E) BSE image of magnetite (Mag)–ilmenite (Ilm) exsolution; the groundmass is quartz–alkali feldspar graphic intergrowths.

DR1). The primary rock-forming minerals are mostly zoned plagioclase feldspar ($An_{41}Ab_{59}$–$An_{18}Ab_{82}$; Fig. 4A), zoned diopside (Fe^{2+}/Mg from 0. 46 in cores to 0.82 at rims; Table DR3 (see footnote 1); Fig. 4B), and ilmenite ($Ti_{0.96–1.00}Fe_{0.90–1.00}Mn_{0.04–0.07}O_3$), intergrown with Ti-bearing magnetite ($Fe^{2+}_{1.08–1.13}Fe^{3+}_{1.69–1.80}Ti_{0.09–0.14}O_4$; Table DR3; Figs. 4B–4C, and 4E). Fluorapatite and baddeleyite are common accessory minerals. Pyrite and chalcopyrite grains were noted as inclusions in pyroxene. The metamorphic overprint is observed by the partial to complete replacement of pyroxene (diopside) by amphibole (actinolite) and rims of ferrian-ferro-hornblende (Figs. 4A–4B; Table DR3). Further evidence of metamorphic alteration is provided by secondary Al-bearing titanite rims on ilmenite and ilmenite-magnetite intergrowths (Fig. 4D). Locally, secondary biotite (Ti = 0.37–0.43 a.p.f.u.; #fm = 0.64–0.67; Table DR3) was formed at the expense of opaque minerals (Fig. 4B). Late chlorite-epidote veins cut the rocks. The metamorphic alteration is typical of greenschist facies metamorphic conditions. Samples also show secondary, low-temperature alteration manifest by the sericitization of plagioclase feldspar and chloritization of mafic silicates and aluminosilicates. The least altered samples are PRGE and AM1, while the other two samples show pervasive alteration (Table DR1). Sample PRGE displayed graphic intergrowths of quartz and alkali feldspar ($Or_{79–56}$, $Ab_{36–17}An_{1–5}$), forming a groundmass between the clusters of mafic phases (Figs. 4C and 4E).

Whole-Rock Major and Trace Geochemistry

Whole-rock major and trace element compositions for the studied mafic sills and dike are listed in Table DR4 (see footnote 1). Data from previous studies (Crow and Condie, 1988; Marsh et al., 1992; Nelson et al., 1992; Meier et al., 2009; Klausen et al., 2010; Gumsley et al., 2016; Meintjes and van der Westhuizen, 2018b) are used for comparison and are shown in Table DR5 (see footnote 1). Data were filtered using an LOI of less than 10% to account for extensive alteration. A thorough review of the geochemistry and petrogenesis of the Ventersdorp Supergroup can be found in Humbert et al. (2019). The mafic sills in this study (AM1 and VJ1) straddle the basalt and the basaltic andesite/andesite fields in the Zr/Ti-Nb/Y classification diagram (Fig. 5A; Pearce, 1996, after Winchester and Floyd, 1977), and are similar to the Klipriviersberg Group basalts and Kopenang dikes, with the lowest Nb/Y and Zr/Ti. The mafic sill PRGE and mafic dike ENED08 are within the basalt and basaltic andesite/andesite range of the Platberg Group volcanic rocks (and Rykoppies Dike Swarm), which are bimodal in Zr/Ti and show greater Zr/Ti in the dacites/rhyolites of the Makwassie Formation. The Allanridge Formation basaltic andesites have a slightly higher Nb/Yb but are equivalent to the lower Zr/Ti grouping from the Platberg Group. The White Mfolozi Dike Swarm, however, is geochemically distinct from the other groupings, having lower Zr/Ti and Nb/Yb. In the AFM diagram (Irvine and Baragar, 1971), samples AM1 and VJ1 and the basalts of the Klipriviersberg Group and the Kopenang dikes plot in the field of tholeiitic basalts with slight calc-alkaline affinities (Fig. 5B). Samples PRGE and ENED08 again show more similarities to the Platberg Group mafic volcanic rocks, Rykoppies Dike Swarm, and Allanridge Formation basaltic andesites, which have

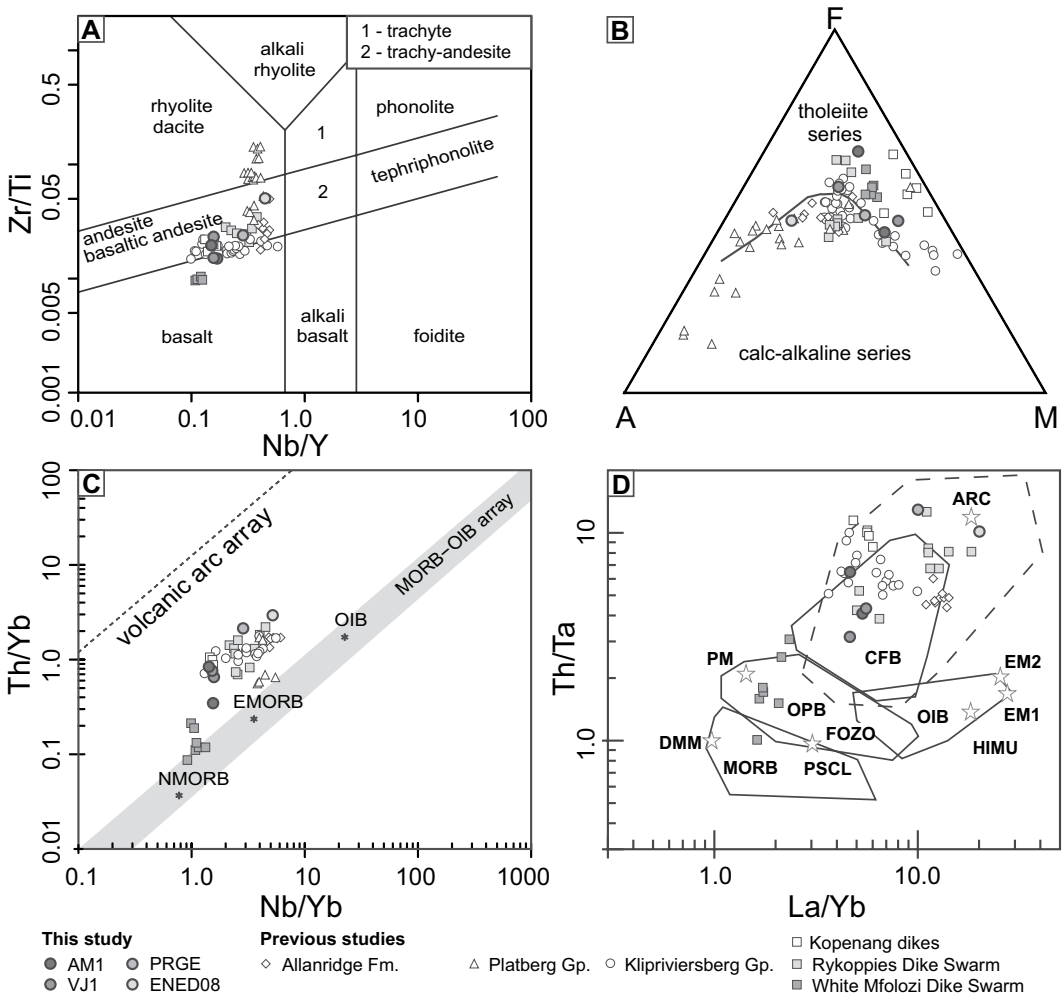

Figure 5. Trace element classification of mafic units. (A) Zr/Ti-Nb/Y classification diagram (Pearce, 1996, after Winchester and Floyd, 1977). (B) AFM diagram (Irvine and Baragar, 1971), $Na_2O + K_2O$ (A), Fe_2O_3* = Fe (total) expressed as Fe_2O_3 (F), and MgO (M). (C) Th/Yb–Nb/Yb diagram of Pearce (2008) for mafic units. NMORB—normal mid-ocean ridge basalt; EMORB—enriched mid-ocean ridge basalt; OIB—ocean island basalt. (D) Th/Ta–La/Yb diagram showing fields for main basalt types and locations of reservoirs; OPB—ocean-plateau basalt; ARC—arc-related; OIB—ocean island basalt; CFB—continental flood basalt; MORB—mid-ocean ridge basalt; PM—primitive mantle; DMM—depleted MORB mantle; PSCL—post-Archean sub-continental lithosphere; HIMU—MORB and OIB with high μ-value (μ = $^{238}U/^{204}Pb$); EM1—enriched mantle 1; EM2—enriched mantle 2; FOZO—focal zone mantle, which is only approximately located. Diagram modified by Ernst (2014) from Condie (2003). Data from previous studies are given in Table DR5 (see footnote 1).

a more calc-alkaline differentiation trend. Using the Th/Yb-Nb/Yb diagram (Pearce, 2008), AM1 and VJ1 are in close proximity to the Kopenang dikes and the Klipriviersberg Group basalts, whereas samples PRGE and ENED08 plot near the mafic volcanic rocks of the Platberg Group, Rykoppies Dike Swarm, and Allanridge Formation basaltic andesites (Fig. 5C). These samples show greater Th/Yb than the mid-oceanic ridge basalt–oceanic island basalt (MORB-OIB) array of oceanic basalts toward the modern volcanic arc array except for the White Mfolozi Dike Swarm, which plots in the MORB–OIB array. Th/Yb is slightly higher in the Platberg Group volcanic rocks, Rykoppies Dike Swarm, and Allanridge Formation basaltic andesites as well as in the dike (ENED08) and sill (PRGE) in this study, compared to the Klipriviersberg Group basalts and Kopenang dikes, including the mafic sills (AM1 and VJ1). Finally, in the Th/Ta–La/Yb diagram (Fig. 5D; Ernst, 2014, after Condie, 2003), samples AM1 and VJ1, including the Klipriviersberg Group basalts and Allanridge Formation basaltic andesites, plot in the continental flood basalt (or CFB field). However, samples from Allanridge Formation basaltic andesites and Rykoppies Dike Swarm, as well as ENED08 and PRGE, have higher La/Yb. The Kopenang dikes have similar values of La/Yb as the Klipriviersberg Group basalts, as well as the VJ1 and AM1 samples, but have higher Th/Ta values, which results in a shift of their location above the CFB field. Samples ENED08 and PRGE have a higher Th/Ta and La/Yb than samples VJ1 and AM1 and plot above the Platberg Group volcanic rocks. At this time, samples from the White Mfolozi Dike Swarm are clearly geochemically distinct from any other unit on the Kaapvaal Craton.

In the chondrite normalized REE diagram and the primitive mantle normalized multi-element plot (Figs. 6A–6D; McDonough and Sun, 1995), samples AM1 and VJ1 are broadly similar to the Klipriviersberg Group basalts and Kopenang dikes. These samples are slightly enriched in light REE relative to heavy REE with no significant anomalies. PRGE and ENED08, however, have elevated levels of REE compared to AM1 and VJ1 and the Klipriviersberg Group basalts and Kopenang dikes. Sample PRGE has a diagnostic enriched REE pattern like that of the Platberg Group volcanic rocks and especially the Makwassie Formation rhyolites and dacites, whereas ENED08 has a similar pattern but is only slightly more enriched as compared to VJ1 and AM1, comparable to the Rykoppies Dike Swarm and the Allanridge Formation basaltic andesites. Only PRGE shows a negative Eu anomaly, and both PRGE and ENED08 are more enriched in light REE compared to heavy REE. Excluding the mobile elements such as Cs, Rb, Ba, Th, and U, all samples have negative Nb and Ta anomalies, as well as negative Ti and slightly negative Eu anomalies.

U-Pb Baddeleyite Geochronology

The water-based separation process of Söderlund and Johansson (2002) yielded ~40

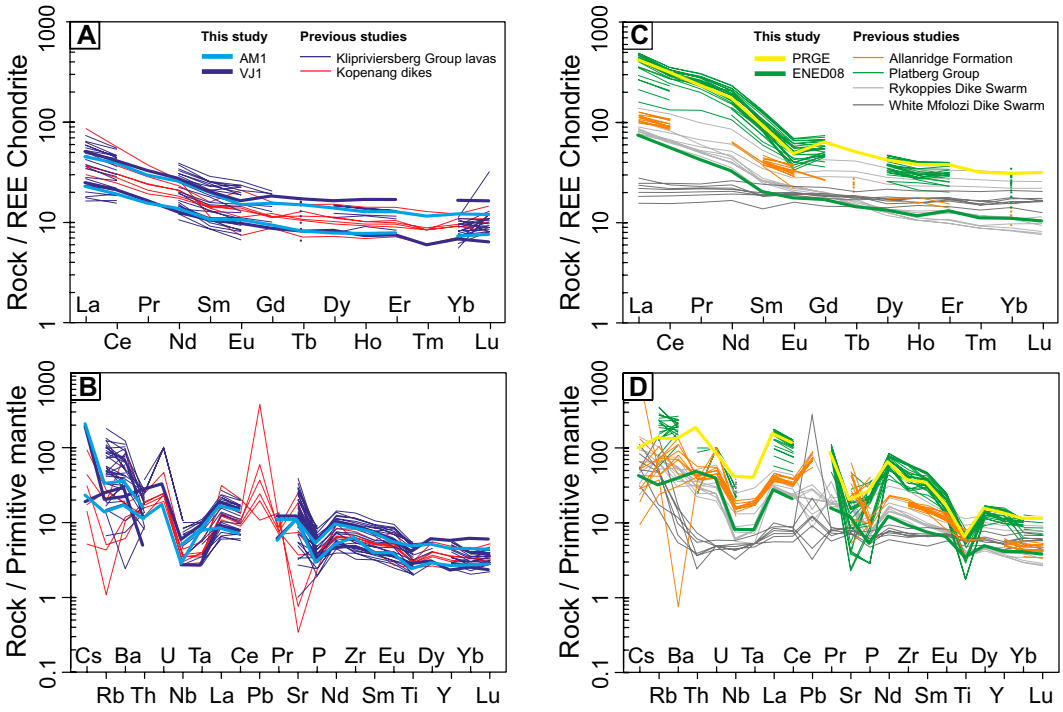

Figure 6. Trace element data for mafic units. (A, C) Chondrite-normalized rare earth element (REE) diagram. (B, D) Primitive mantle-normalized diagram. Normalization values from McDonough and Sun (1995). Data from previous studies are given in Table DR5 (see footnote 1).

grains of baddeleyite each for VJ1 and PRGE, and 30 grains for AM1, whereas only 20 grains of ENED08 were recovered. The best-quality grains analyzed in the VJ1, AM1, and ENED08 samples were light brown and generally clear with some slight to moderate frostiness with a length of between 50 µm and 60 µm for VJ1 and ~30 µm for AM1. ENED08 baddeleyite grains were between 20 µm and 30 µm long. Sample PRGE had baddeleyite grains that were dark brown and generally clear with some slight frostiness with lengths of ~40 µm. U and Pb isotopic measurements are listed in Tables DR6 and DR7 (see footnote 1), and data are plotted on Wetherill concordia diagrams in Figures 7 and 8.

ID-TIMS

Four fractions of baddeleyite from VJ1 were analyzed, which were composed of between two and three baddeleyite grains each (Fig. 7A). Regression of these fractions produced a precise upper intercept date of 2787 ± 2 Ma (mean square of weighted deviates [MSWD] = 1.5). Three fractions are between 2% to 1% discordant and a fourth fraction is 6% discordant, likely due to zircon alteration. The most discordant fraction constrains the lower intercept of 295 ± 98 Ma. A weighted mean $^{207}Pb/^{206}Pb$ date of the three least discordant fractions is 2785 ± 1 Ma (MSWD = 0.67). The fourth fraction is excluded because it is not within error of the $^{207}Pb/^{206}Pb$ dates of the other three fractions. Two fractions of AM1, composed of six baddeleyite grains each, produced a preliminary upper intercept date of 2789 ± 4 Ma (Fig. 7B), which is within error of the date of VJ1. Regression yields a preliminary lower free intercept date of 106 ± 190 Ma. The two fractions were 5% and 2% discordant, with $^{207}Pb/^{206}Pb$ dates between ca. 2788 Ma and ca. 2786 Ma. For sample ENED08, three baddeleyite fractions were analyzed, with three grains in each (Fig. 7C). Free regression yields upper and lower intercept dates of 2729 ± 5 Ma and 228 ± 57 Ma, respectively (MSWD <0.1). Two fractions plot between 6% and 5% discordant and have $^{207}Pb/^{206}Pb$ dates between ca. 2723 Ma and ca. 2722 Ma, and a third fraction is 16% discordant, likely as a result of zircon alteration, and constrains the lower intercept.

Sample PRGE yielded an upper intercept date of 2727 ± 3 Ma and a lower intercept date of 540 ± 280 Ma (MSWD = 0.71) from analysis of four fractions of baddeleyite (Fig. 7D). The discordance varies between 10% and 0%, with the three least discordant fractions being between 1% and 0% discordant. A weighted mean $^{207}Pb/^{206}Pb$ age calculated on these three least discordant dates is 2724 ± 7 Ma (MSWD = 3.3). The fourth fraction is excluded due to not being within error of the $^{207}Pb/^{206}Pb$ dates of the other three fractions.

LA-ICPMS

Analytical results from the Phalaborwa Complex reference material (Heaman, 2009) are presented in Table DR7 (see footnote 1). No significant difference was observed between $^{207}Pb/^{206}Pb$ ratios of VJ1 measured in the sequence, but the isotopic data show variable discordance (between ~17% and ~1%), forming a discordant array in a Wetherill concordia diagram (Fig. 8A). Using all data (Table DR8; see footnote 1), we obtain an upper intercept date of 2799 ± 15 Ma (MSWD = 3.4) and a weighted mean $^{207}Pb/^{206}Pb$ date of 2796 ± 6 Ma (MSWD = 3.2; Fig. 8B).

Difficulties in determining the true U-Pb dates of grains analyzed using LA–ICPMS might arise from difficulties with correction of common Pb. In the presented data, the average mass 204 background signal was relatively high, around 1900 counts per second, which increases the risk that small amounts of common Pb cannot be detected. When detecting isotopes close to the detection limit, it is not possible to quantify concentrations; however, by plotting the $^{206}Pb/^{204}Pb$ against common Pb corrected and uncorrected $^{207}Pb/^{206}Pb$ dates, we observe an increasing age difference for analyses with low $^{206}Pb/^{204}Pb$, which mainly shows up in decreasing common Pb corrected dates. This supports the idea that some grains contain a small amount of common Pb but also that we seemingly overcorrect the data, as observed when $^{206}Pb/^{204}Pb$ ratios are below 9000. Using all uncorrected data, we obtain an upper intercept date of 2799 ± 15 Ma (MSWD = 3.4) and a weighted mean $^{207}Pb/^{206}Pb$ date of 2796 ± 6 Ma (MSWD = 3.2). Using only uncorrected data from analyses with $^{206}Pb/^{204}Pb$ above 9000, we

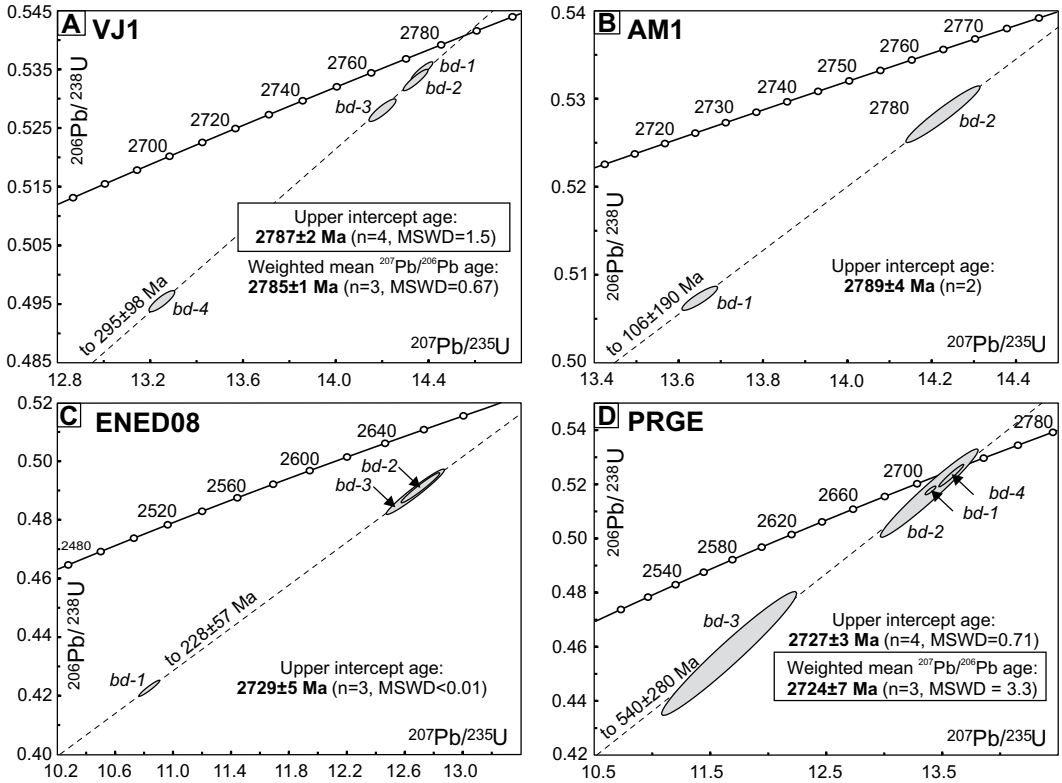

Figure 7. Wetherill concordia diagrams of U-Pb ID–TIMS analyses, with $^{206}Pb/^{238}U$-$^{207}Pb/^{235}U$ isotopic ratios of the analyzed baddeleyite fractions. (A) sample VJ1; (B) sample AM1; (C) sample ENED08; (D) sample PRGE. All data point error ellipses and age calculations are shown at 2σ; ^{238}U and ^{235}U decay constant uncertainties are ignored. MSWD—mean square of weighted deviates; *n* refers to the total number of fractions analyzed. Error ellipse symbols (*bd-x*) refer to the fractions analyzed and shown in Table DR6 (see footnote 1). Preferred ages given in rectangles.

obtain an upper intercept date of 2798 ± 12 Ma (MSWD = 1.9) and a weighted mean $^{207}Pb/^{206}Pb$ date of 2793 ± 7 Ma (MSWD = 1.7; Fig. 8B). As observed, there is, within the limits of uncertainty, no significant difference between these age estimates. We, however, prefer to use the data that are arguably least affected by common Pb, and thus our best date estimate of VJ1 is 2798 ± 12 Ma, using the upper intercept, as with the ID-TIMS data.

DISCUSSION

Crystallization Ages by ID–TIMS and LA–ICPMS on Baddeleyite

Regression of the U-Pb ID–TIMS data for VJ1 yields an upper intercept date of 2787 ± 2 Ma (MSWD = 1.5) and is within analytical uncertainty of the LA–ICPMS result as well as the preliminary AM1 date of 2789 ± 4 Ma, both of which are also obtained by free regression. This is preferred age over a weighted mean $^{207}Pb/^{206}Pb$ age on the three least discordant analyses at 2785 ± 1 Ma (MSWD = 0.67), as no data overlap the concordia, making the weighted mean date a minimum age. Although the lower intercept is close to 0 Ma, which indicates recent Pb disturbance, it is still beyond uncertainty at 295 ± 98 Ma, and therefore an isotopic disturbance at an earlier time is possible. This is interpreted as likely belonging to the Karoo magmatic event at 183–179 Ma (Duncan et al., 1997). The relatively precise 2787 ± 2 Ma date is our preferred crystallization age, since ID–TIMS normally allows for robust common-Pb correction. Noteworthy is that the discordance of ID–TIMS fractions is ~3%, i.e., much less than for the LA–ICPMS analyses. The crystallization age of ENED08 is also interpreted as 2729 ± 5 Ma (MSWD < 0.01) using a free regression, as no analyses overlap with the concordia, with Pb disturbance again likely attributed to Karoo magmatism. The upper intercept date of PRGE is 2727 ± 3 Ma (MSWD = 0.71). However, a weighted mean $^{207}Pb/^{206}Pb$ date on the three least discordant fractions, which overlap the concordia, is 2724 ± 7 Ma (MSWD = 3.3). The weighted mean $^{207}Pb/^{206}Pb$ date is thus our preferred crystallization age for PRGE.

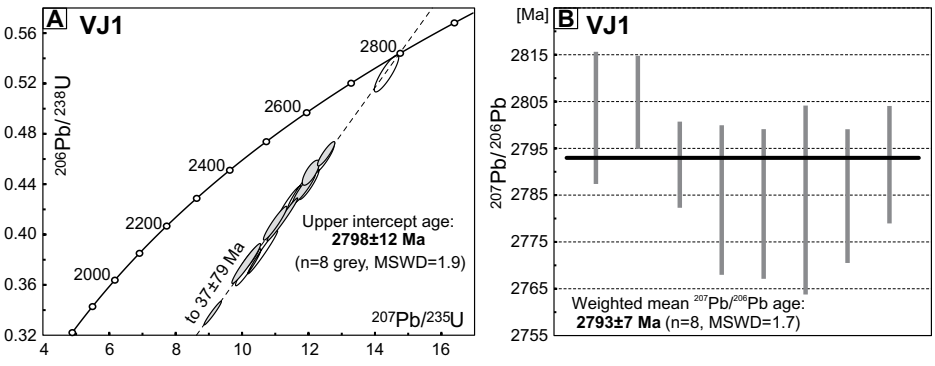

Figure 8. U-Pb laser ablation-inductively coupled plasma mass spectrometry (LA–ICPMS) baddeleyite analyses for sample VJ1. (A) Wetherill concordia diagram with $^{206}Pb/^{238}U$-$^{207}Pb/^{235}U$ isotopic ratios of the analyzed baddeleyite fractions. All data point error ellipses and age calculations are shown at 2σ, and ^{238}U and ^{235}U decay constant uncertainties are ignored. Data are presented in Table DR8 (see footnote 1). (B) Weighted mean age, with 2σ uncertainties for each analysis. MSWD—mean square of weighted deviates; *n* refers to the total number of spots analyzed.

Source of Magma

The incompatible element patterns of all the magmatic events presented in Figure 6 are different, but with the exception of the White Mfolozi Dike Swarm, they all show "subduction-related" or "arc-like" signatures (e.g., Pearce, 2008; Ernst, 2014; O'Neill and Jenner, 2016; Humbert et al., 2018; 2019) that are notably marked by negative Nb and Ta anomalies. These signatures are common in many Archean and Paleoproterozoic mafic rocks of the Kaapvaal Craton (e.g., O'Neill and Jenner 2016; Humbert et al., 2018; 2019) and in other intraplate events (including LIPs) in the rest of the world (e.g., Pearce, 2008; Ernst, 2014). These events also plot higher Th/Yb and Th/Nb values than the MORB-OIB array (Fig. 5C). According to Pearce (2008), this preferential enrichment in Th over Nb may either indicate crustal contamination or assimilation of the magma and/or a lithospheric mantle source that was fluid-metasomatized by past subduction. Substantial crustal contamination actually has been inferred through whole-rock Sm-Nd isotopic data in the case of the Platberg Group (average $\varepsilon Nd_{2720}Ma = -3.4$) and Allanridge Formation (average $\varepsilon Nd_{2700}Ma = -3.0$), with an average $\varepsilon Nd_{2780}Ma = 0$ for the source of the Klipriviersberg magmas probably also possibly contaminated to a lesser extent (Humbert et al., 2019). Note that no isotopic data exist for the other events so far. In addition, the quartz and alkali feldspar groundmass in the PRGE sample can be interpreted as the result of local mixing-mingling phenomena (e.g., Burda et al., 2011) from assimilation of silica-rich material. It can also simply represent the highly fractionated portions of rift-related intracontinental basaltic magma.

Samples from the White Mfolozi Dike Swarm are clearly geochemically distinct from any other unit on the Kaapvaal Craton (Figs. 5 and 6). They notably present lower Th/Yb, Nb/Yb, Th/Ta, and La/Yb ratios, as well as "flat" and moderately enriched signatures compared to chondrite/primitive mantle in REE/trace-element diagrams. The White Mfolozi Dike Swarm samples plot close to primitive mantle in Figures 5C and 5D and might be from such a source. On the contrary, they also may have been generated from a depleted mantle source (i.e., NMORB-like) that later underwent minor crustal contamination.

Chronostratigraphic Constraints on the Development of the Ventersdorp Supergroup

The Klipriviersberg Large Igneous Province

The herein dated 2787 ± 2 Ma and 2789 ± 4 Ma mafic sills VJ1 and AM1 are the first documented occurrence of this magmatic event from the central region of the Kaapvaal Craton (Fig. 9). These sills are situated stratigraphically beneath the Klipriviersberg Group flood basalts of the Ventersdorp Supergroup in the Witwatersrand Supergroup and are interpreted as likely related to them. Further, these mafic sills closely resemble the flood basalts of the Klipriviersberg Group geochemically (Figs. 5 and 6; e.g., Winter, 1976; Marsh et al., 1992; Humbert et al., 2019). Meier et al. (2009) has already shown the similar geochemical

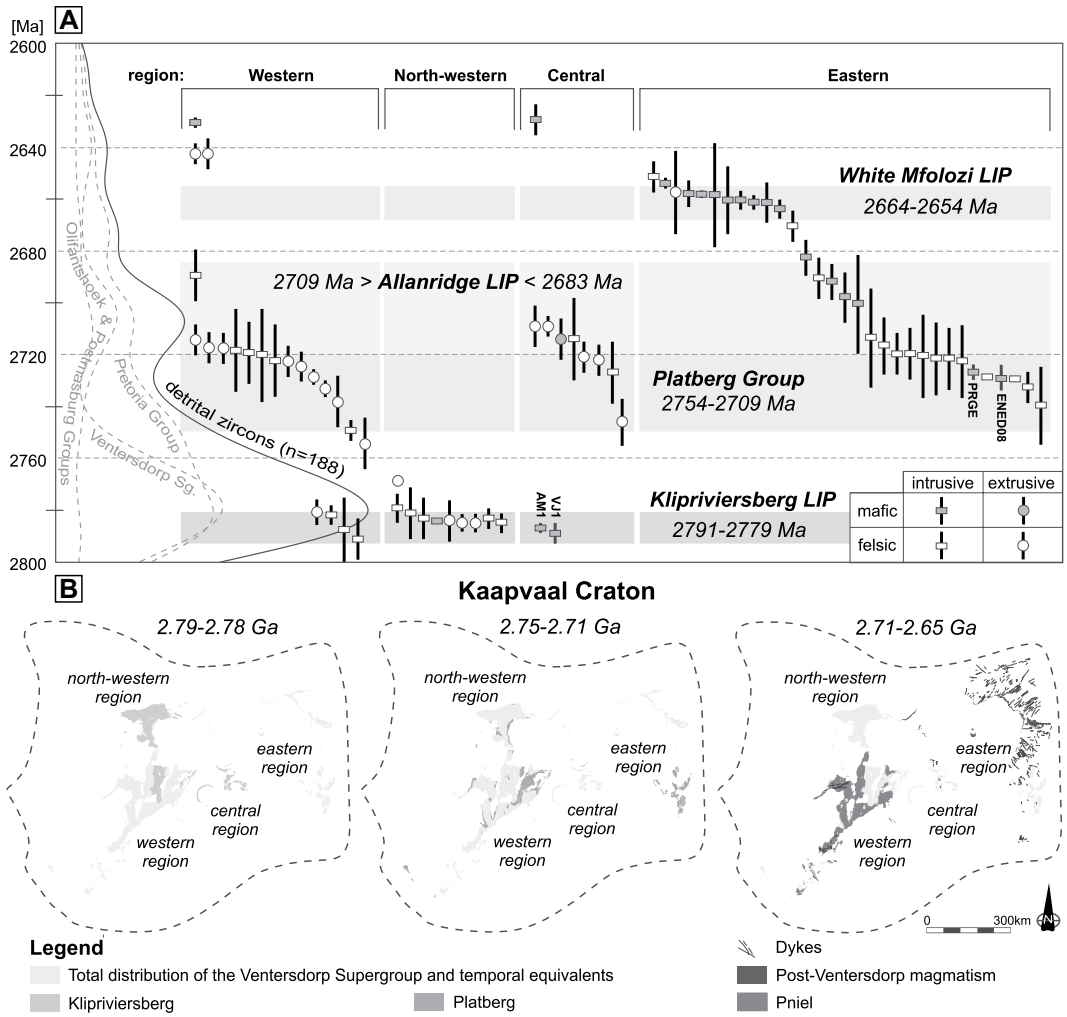

Figure 9. (A) Summary of U-Pb zircon and baddeleyite age determinations of felsic and mafic rocks, both intrusive and extrusive from eastern southern Africa, divided into four regions. Data sources are given in Table 1 and Table DR9 (see footnote 1). Data were filtered, and only ages with 2σ less than 20 Ma are plotted. Probability density distribution diagrams are shown for detrital zircon ages from the Postmasburg Group, the Pretoria Group, and Ventersdorp Supergroup. Data sources are given in Table DR10 (see footnote 1). Only results with discordance less than 5% are plotted. Uncertainties in age are given at 2σ; *n* refers to the total number of data points analyzed. (B) Neoarchean development and distribution of the Ventersdorp Supergroup and related units at 2791–2779 Ma, 2754–2709 Ma, and between 2709 and 2654 Ma on the Kaapvaal Craton. LIP—large igneous provinces.

characteristics of mafic feeders to the Klipriviersberg Group flood basalts in the form of the Kopenang dikes intruding the Witwatersrand Supergroup in the same area (Fig. 1). Therefore, it is reasonable to interpret that the mafic sills AM1 and VJ1 analyzed in this study belong to a single magmatic system represented by mafic intrusions that fed the overlying flood basalts of the Klipriviersberg Group.

As shown in Figure 9, we now recognize a widespread 2791–2779 Ma magmatic event across the central, western, and northwestern regions of the Kaapvaal Craton. The mafic sills from the central region of the Kaapvaal Craton in this study, AM1 and VJ1, are coeval with the bimodal volcanic Kanye Formation and its plutonic equivalent, the Gabarone Complex granites. The Kanye Formation has been considered a protobasinal or precursor phase to the Ventersdorp Supergroup in the Swartruggens Trough (Tyler, 1979; Ernst, 2014). The nearby Derdepoort Formation and Modipe Complex gabbro was dated to 2782 ± 5 Ma and 2784 ± 1 Ma, respectively (Table 1; Wingate, 1998; Denyszyn et al., 2013). These units were originally correlated with the Klipriviersberg Group flood basalts and other units of the Ventersdorp Supergroup (Tyler, 1979). Similarly aged units are documented in the Amalia–Kraaipan granite-greenstone terrane of the western and northwestern regions of the Kaapvaal Craton (Figs. 9A and 9B). These include the Mosita, Mmathete, and "red" granites, as well as the Turfloop and Rooibokvlei granites in the Makoppa Dome (e.g., Grobler and Walraven, 1993; Moore et al., 1993; Mapeo et al., 2004; de Kock et al., 2012; Denyszyn et al., 2013; Ernst, 2014). This magmatic event is also recorded in detrital zircon data from the Ventersdorp and Transvaal supergroups (Figs. 9A and 9B; Tables DR9 and DR10; see footnote 1).

Furthermore, the ages proposed for the Klipriviersberg Group flood basalts in this study do not agree with the 2714 ± 16 Ma age obtained by Armstrong et al. (1991) from the type locality of the Klipriviersberg Group flood basalts. This is the only volcanic event occurring in the region of the mafic sills dated in this study other than the ca. 2914 Ma Crown Formation lava of the Witwatersrand Supergroup (Armstrong et al., 1991; Fig. 9A). However, the age presented by Armstrong et al. (1991) for the Klipriviersberg Group flood basalts has been questioned by Wingate (1998), de Kock et al. (2012), Cornell et al. (2017), and Humbert et al. (2019). A recalculation of the Armstrong et al. (1991) isotopic data using the least discordant analyses at ca. 2.7 Ga and ca. 1.0 Ga results in an upper intercept date of 2757 ± 57 Ma and a lower intercept date of 1082 ± 140 Ma. This result, as originally shown by Wingate (1998), indicates that the magmatic/metamorphic event that formed the younger ca. 1.0 Ga generation of zircons may have affected the ca. 2.7 Ga zircons and should be regarded as a minimum age of crystallization for the flood basalts. Recent geochronological studies on the Platberg Group (in the Makwassie Formation) and one of its stratigraphic equivalents (i.e., the Hartswater Group) also add temporal constraints on the age of the Klipriviersberg Group, indicating an older age (e.g., de Kock et al., 2012; Cornell et al., 2017). Furthermore, Barton et al. (1989) analyzed detrital zircons from the Venterspost Formation, which constitutes the base of the Klipriviersberg Group, and obtained a maximum age of 2780 ± 5 Ma for deposition of the formation from the youngest concordant zircon grains.

The magmatic event described above meets the criteria for a LIP, as specified by Ernst (2014). As illustrated in Figure 9, we can now redefine this event to encompass the Klipriviersberg Group flood basalts and coeval mafic sills, the Kanye and Derdepoort bimodal volcanic rocks, and the temporally related Gabarone Complex and Modipe Complex granites and gabbros as well as granites farther afield to the west (Fig. 9B). The LIP had an area of ~250,000 km^2, with the thickness of the flood basalt package up to 2 km. Further material from the magmatic province has likely eroded away, as shown by the extensive detrital zircon spectra peak at ca. 2.78 Ga. An age range for all units belonging to this newly defined Klipriviersberg LIP is 2791–2779 Ma, although through more modern methodology, this age range can likely be narrowed further. Additionally, the lack of any intervening sedimentary layers or unconformities in the flood basalts provides further evidence of the short-lived duration of the magmatic event.

The Platberg Volcanic Province

Following a magmatic hiatus from the Klipriviersberg LIP, large-scale rifting, sedimentation, and volcanism dominated the western and central Kaapvaal Craton between 2754 Ma and 2709 Ma (de Kock et al., 2012; Cornell et al., 2017). In the eastern Kaapvaal Craton, numerous granites were emplaced simultaneously (e.g., Hofmann et al., 2015), which Taylor et al. (2010) argued were likely related to the extension and magmatism that deposited the Ventersdorp Supergroup (Figs. 9A and 9B; Tables DR9 and DR10). In this study, the mafic sill PRGE from the southeastern part of the Kaapvaal Craton intruding into the Pongola Supergroup was dated to 2724 ± 7 Ma, and thus it is coeval with this widespread magmatic event. Geochemically, this sill resembles volcanic rocks within the Platberg Group, specifically the Makwassie Formation (Figs. 5 and 6). Near the sill, the Amsterdam Formation is the only unit with which it may be linked. The Amsterdam Formation unconformably overlies the Pongola Supergroup and is a volcanic succession composed of the Gobosha Member dacites near Amsterdam and the Vaalkop Member rhyolites near Piet Retief (Hammerbeck, 1982). The sill geologically and geochemically resembles the Gobosha dacites of the Amsterdam Formation (Hammerbeck, 1982), and therefore it is hypothesized as a likely part of a feeder system to the volcanic rocks of the Amsterdam Formation. This interpretation implies that the Amsterdam Formation is the easternmost equivalent of the Platberg Group (Fig. 9B). Additionally, farther to the east in the Mkondo Suite, leucosomes dated to 2730 ± 5 Ma have been reported to date granulite facies metamorphism (Taylor et al., 2010).

To the south of the dated sill, our age of 2729 ± 5 Ma for ENED08 on a coeval east-northeast–trending dike establishes a newly identified dike swarm on the southeasternmost part of the Kaapvaal Craton. This dike swarm, which we name the "Ulundi Dike Swarm" (Figs. 1 and 3), is the first recognized dike swarm associated with the Platberg Group of the Ventersdorp Supergroup and extends this magmatic event further to the southeast. The ENED08 dike is cut by plagioclase megacrystic northeast-trending dikes of the 2664–2654 Ma White Mfolozi Dike Swarm (Gumsley et al., 2016) as well as by a mafic sheet dated at 2420 ± 3 Ma (Gumsley et al., 2017).

Using the new age constraints presented in this study of 2729 ± 5 Ma for ENED08 and 2724 ± 7 Ma for PRGE, and age constraints of 2733–2724 Ma in de Kock et al. (2012) and 2720 ± 2 Ma in Cornell et al. (2017), the Platberg volcanic province (or possibly a LIP pulse of a combined Platberg–Allanridge LIP) is constrained to between ca. 2754 Ma and ca. 2709 Ma. For the Makwassie Formation, the Cornell et al. (2017) age of 2720 ± 2 Ma replaces the original 2709 ± 8 Ma age presented by Armstrong et al. (1991). A detrital zircon-spectra peak again provides evidence of magmatism and erosion at ca. 2.71 Ga.

The Allanridge Large Igneous Province

These new data for samples ENED08 and PRGE help to refine the minimum and maximum age constraints on the Allanridge Formation basaltic andesites, which unconformably overlie the Platberg Group along with the Bothaville Formation (both part of the Pniel Group). The Allanridge Formation basaltic andesites are sufficiently voluminous to be defined as a LIP according to Ernst (2014), being over 200,000 km^2 in area and up to 1 km thick. Age constraints on the Allanridge LIP bracket its

deposition between ca. 2709 Ma, which is the age of the underlying Makwassie Formation of the Platberg Group (Cornell et al., 2017), and ca. 2664 Ma, which corresponds to the age of the Buffelsfontein Group in the overlying proto-basins of the Transvaal Supergroup (Barton et al., 1995).

However, the Rykoppies Dike Swarm, emplaced between ca. 2701 Ma and ca. 2664 Ma, may also be linked to the Allanridge LIP and appears geochemically similar (Figs. 5 and 6). This mafic magmatism documents peaks at 2701–2692 Ma, 2686–2683 Ma, and 2664–2659 Ma (Gumsley et al., 2016). Reinterpretation of the complex discordant U-Pb isotopic data and Pb loss histories of these dike swarms appears to indicate two magmatic events at 2701–2683 Ma and 2664–2654 Ma using only the least discordant U-Pb baddeleyite isotopic data from the Rykoppies and White Mfolozi dike swarms. If this is correct, the age of the Allanridge LIP may reflect this older pulse at 2701–2683 Ma in the Rykoppies Dike Swarm, with further magmatism at 2664–2654 Ma represented by the geochemically distinct White Mfolozi Dike Swarm, which is coeval to parts of the Rykoppies Dike Swarm (despite being geochemically different) and volcanism and renewed rifting in proto-basinal fills to the Transvaal Supergroup, such as the bimodal volcanic rocks of the Buffelsfontein Formation at 2664 ± 1 Ma (Barton et al., 1995). The White Mfolozi Dike Swarm may then be regarded as a separate magmatic event, potentially another LIP, especially when including coeval parts of the Rykoppies Dike Swarm. The White Mfolozi Dike Swarm has a unique geochemical signature but has an approximately orthogonal linear trend to the Rykoppies Dike Swarm, which is radiating (Fig. 1). While the White Mfolozi Dike Swarm could represent part of a separate linear or radiating swarm, we speculate that the White Mfolozi Dike Swarm could alternatively be evidence for a giant circumferential swarm (Buchan and Ernst 2018, 2019) that circumscribes the plume center at the focus of the Rykoppies Dike Swarm.

LIPs and the Ventersdorp Supergroup

In summary, Ventersdorp magmatism can be divided into distinct volcanic/magmatic events, some of which are of LIP scale, including the 2791–2779 Ma Klipriviersberg LIP and the 2701–2683 Ma Allanridge LIP, which are separated from the 2664–2654 Ma White Mfolozi/Rykoppies magmatic province, which may also be a LIP. Despite the unconformity between the Platberg Group and the Pniel Group, the Allanridge LIP was closely preceded by the 2754–2709 Ma Platberg volcanic province, which is composed of a mixed succession of sedimentary and bimodal volcanic rocks. The Platberg Group was, therefore, likely genetically related to a mantle plume responsible for the emplacement of the Allanridge LIP beneath the lithosphere, making the plume distinctly pulsed (with fractionation or arc-related magmatism, with a crustal contribution, as seen from geochemistry; Humbert et al., 2019). The mantle plume center for the Allanridge LIP is well defined by the radiating Rykoppies Dike Swarm. In addition, the associated Ventersdorp rift zone trends approximately from this plume center, suggesting that this rifting was in part coeval with the Allanridge LIP. The location of a plume center for the 2791–2779 Ma Klipriviersberg LIP and 2664–2654 Ma White Mfolozi volcanic province remains unconstrained.

Implications for the Age of Gold Deposition within the Witwatersrand Supergroup

The 2787 ± 2 Ma and 2789 ± 4 Ma mafic sills reported in this study intrude and crosscut the gold-bearing Witwatersrand Supergroup successions, indicating that the placer gold deposits must predate the mafic dikes and sills as suggested by Meier et al. (2009). This makes the minimum depositional age for placer gold and the Witwatersrand Supergroup greater than ca. 2.79 Ga and is in agreement with the ca. 2.78 Ga and ca. 2.76 Ga diagenetic ages reported from xenotime (England et al., 2001; Kositcin et al., 2003) as well as a ca. 2.78 Ga detrital zircon age for the Venterspost Formation of the Klipriviersberg Group, which conformably overlies the Witwatersrand Supergroup (Barton et al., 1989). This further confirms the approximate minimum and maximum age constraints for the cessation of the Witwatersrand Supergroup deposition and the initiation of the Ventersdorp Supergroup. The Venterspost Formation was deposited conformably onto the Witwatersrand Supergroup, with the sedimentary rocks still unconsolidated with the eruption of the Klipriviersberg Group flood basalts (Chunnett, 1994). Diagenesis occurred between ca. 2.78 Ga and ca. 2.76 Ga (England et al., 2001; Kositcin et al., 2003). This has implications for gold metallogeny, indicating that the Witwatersrand Supergroup sedimentary rocks were deposited within a maximum timespan of ~180 m.y., as opposed to the previously suggested maximum timespan of ~256 m.y., dating gold metallogeny to ca. 2.78 Ga (Armstrong et al., 1991; Meier et al., 2009).

Tectonic Model

Using the chronostratigraphic constraints above (Figs. 9A and 9B), at 2791–2779 Ma, large amounts of magmatic material were preserved in the central and northwestern regions of the Kaapvaal Craton, such as the Klipriviersberg LIP. This LIP incorporates the Klipriviersberg flood basalts that flowed across the central Kaapvaal Craton and the Kanye and Derdepoort basalts and rhyolites on the northwestern Kaapvaal Craton. This was accompanied by the emplacement of anorogenic granites, which were likely produced from crustal melting associated with an underlying mantle plume responsible for the Klipriviersberg LIP (Grobler and Walraven, 1993). These granites were emplaced along the Colesberg and Thabazimbi–Murchison lineaments, which likely reflected suture zones of thin, weaker crust susceptible to higher heat flows (e.g., Ernst, 2014). A mantle plume is shown in LIP-scale magmatism, incorporating mantle-derived komatiites and high-MgO basalts at the base of the Klipriviersberg Group as well as uplift and erosion of unconsolidated Witwatersrand Supergroup and Venterspost Formation sediments before deposition of the Klipriviersberg Group flood basalts.

As extensive, short-lived magmatism of the Klipriviersberg LIP terminated, the impact of the same or potentially a different mantle plume some ~30 m.y. later led to extension and graben development associated with volcanism and sedimentation across the central and western Kaapvaal Craton; this is now preserved as the Platberg Group between ca. 2754 and ca. 2709 Ma. In the southeastern Kaapvaal Craton, this magmatism is also now documented in the 2729 ± 5 Ma east-northeast–trending Ulundi Dike Swarm and possibly in the Amsterdam Formation, which accompanied metamorphism, core complex emplacement, and granite formation in Swaziland and adjacent areas of South Africa. Mafic magmatism in this area is also evident in sills in the Pongola Supergroup dated here to 2724 ± 7 Ma.

As the grabens were filled with the Platberg Group, sedimentation and volcanism continued after a small hiatus in the Pniel Group sometime after ca. 2709 Ma, with basaltic andesites preserved as the Allanridge LIP likely erupted between ca. 2709 Ma and ca. 2683 Ma, which was possibly related to the same mantle plume responsible for the Platberg volcanic province. Once again, the LIP itself, uplift and erosion of the Platberg Group rocks, and emplacement of komatiites and high-MgO basalts at the base of the Allanridge Formation basaltic andesites provide evidence for a mantle plume. These volcanic rocks blanketed the underlying western regions of the Kaapvaal Craton, while mafic dike swarms were emplaced at 2701–2683 Ma on the eastern region of the Kaapvaal Craton in the Rykoppies Dike Swarm. The Rykoppies Dike

Swarm radiates out from a focus underneath the eastern Bushveld Complex and was likely produced by a mantle plume at 2701–2683 Ma (Olsson et al., 2011), if the three pulses of magmatism proposed by Gumsley et al. (2016) are reinterpreted and reduced to two (Olsson et al., 2010, 2011) at 2701–2683 Ma and at 2664–2654 Ma, with the older pulse being responsible for the Allanridge LIP. The 2664–2654 Ma pulse was possibly associated with another LIP and renewed rifting in the so-called proto-basins to the Transvaal Supergroup and the White Mfolozi Dike Swarm, with some magma injected along the same trends as those of the Rykoppies Dike Swarm, possibly under the same stress regime or lines of weakness in the crust. This terminated volcanism on the Kaapvaal Craton during the proto-basinal phases to the Transvaal Supergroup, which included failed rifting.

CONCLUSION

Baddeleyite from two mafic sills interpreted as feeders of Klipriviersberg magmatism, hosted within the Witwatersrand Supergroup on the central Kaapvaal Craton, yields U-Pb ID-TIMS crystallization ages of 2787 ± 2 Ma and 2789 ± 4 Ma. Complementary U-Pb LA–ICPMS analysis of baddeleyite grains from one of the sills yielded an similar crystallization age of 2793 ± 7 Ma. All dates above overlap within error, and a 2791–2779 Ma age is interpreted for emplacement of these sills and the larger Klipriviersberg LIP. Baddeleyite from a mafic sill in the Pongola Supergroup on the southeastern Kaapvaal Craton yielded a crystallization age of 2724 ± 7 Ma. This extends magmatism associated with the Platberg Group farther east to the southeastern Kaapvaal Craton. Additionally, an east-northeast–trending mafic dike from the southeasternmost Kaapvaal Craton, part of the newly defined Ulundi Dike Swarm, produced a U-Pb baddeleyite crystallization age of 2729 ± 7 Ma, which makes it part of the first dike swarm directly related to the Ventersdorp Supergroup (specifically the Platberg Group). Our results extend the 2791–2779 Ma magmatic event into the central Kaapvaal Craton and 2754–2709 Ma magmatism into the southeastern Kaapvaal Craton.

These new data, combined with previous data associated with the 2701–2654 Ma Rykoppies and White Mfolozi magmatism, allow us to distinguish two separate LIPs within the Ventersdorp Supergroup and shortly thereafter: at 2791–2779 Ma in the Klipriviersberg LIP, at 2701–2683 Ma in the Allanridge LIP, and potentially at 2664–2654 Ma in the White Mfolozi Dike Swarm after the formation of the Ventersdorp Supergroup but before formation of the Transvaal Supergroup. The first two LIPs initiated and terminated Ventersdorp Supergroup development across the entire Kaapvaal Craton, which can be associated with magmatism of the Klipriviersberg Group and the Pniel Group, respectively. These LIPs are separated by rifting and graben development with associated sedimentation and bimodal volcanism during the formation of the 2754–2709 Ma Platberg Group during the arrival of the Allanridge mantle plume at the base of the lithosphere. These new ages also allow us to reinterpret the timing of gold deposition within the Witwatersrand Supergroup, with gold deposition in the conglomerates occurring before ca. 2.79 Ga.

ACKNOWLEDGMENTS

The authors would like to thank the staff at GSA Bulletin and editor Rob Strachan for all their assistance throughout the publication process. The authors are also grateful to the detailed and constructive review of Steve Denyszyn. Ashley Gumsley acknowledges financial support through a grant from the National Science Centre, Poland (POLONEZ grant no. UMO-2016/23/P/ST10/02423). This grant has received funding from the European Union's Horizon 2020 research and innovation programme under the Marie Skłodowska-Curie Actions COFUND-2014 (grant no. 665778). Funding for the U-Pb geochronology by De Beers is gratefully acknowledged. Richard Ernst was partially supported by Russian Federation mega-grant 14.Y26.31.0012. Michiel de Kock acknowledges support from the DST-NRF Centre of Excellence in Mineral and Energy Resource Analysis (CIMERA) as well as NRF incentive funding. This article is a contribution to International Geoscience Programme (IGCP) 648: Supercontinents and Global Geodynamics.

REFERENCES CITED

Altermann, W., and Lenhardt, N., 2012, The volcano-sedimentary succession of the Archean Sodium Group, Ventersdorp Supergroup, South Africa: Volcanology, sedimentology and geochemistry: Precambrian Research, v. 214–215, p. 60–81, https://doi.org/10.1016/j.precamres.2012.02.012.

Armstrong, R.A., Compston, W., Retief, E.A., Williams, I.S., and Welke, H.J., 1991, Zircon ion microprobe studies bearing on the age and evolution of the Witwatersrand triad: Precambrian Research, v. 53, p. 243–266, https://doi.org/10.1016/0301-9268(91)90074-K.

Barton, E.S., Compston, W., Williams, I.S., Bristow, J.W., Hallbauer, D.K., and Smith, C.B., 1989, Provenance ages for the Witwatersrand Supergroup and the Ventersdorp contact reef: Constraints from ion microprobe U-Pb ages of detrital zircons: Economic Geology and the Bulletin of the Society of Economic Geologists, v. 84, p. 2012–2019, https://doi.org/10.2113/gsecongeo.84.7.2012.

Barton, J.M., Jr., Blignaut, E., Salnikova, E.B., and Kotov, A.B., 1995, The stratigraphical position of the Buffelsfontein group based on field relationships and chemical and geochronological data: South African Journal of Geology, v. 98, p. 386–392.

Beukes, N.J., and Cairncross, B., 1991, A lithostratigraphic-sedimentological reference profile for the Late Archaean Mozaan Group, Pongola Sequence: Application to sequence stratigraphy and correlation with the Witwatersrand Supergroup: South African Journal of Geology, v. 94, p. 44–69.

Buchan, K.L., and Ernst, R.E., 2018, A giant circumferential dyke swarm associated with the High Arctic Large Igneous Province (HALIP): Gondwana Research, v. 58, p. 39–57, https://doi.org/10.1016/j.gr.2018.02.006.

Buchan, K.L., and Ernst, R.E., 2019, Giant Circumferential Dyke Swarms: Catalogue and Characteristics, *in* Srivastava, R.K., Ernst, R.E., and Peng, P., eds., Dyke Swarms of the World—A Modern Perspective: Amsterdam, Springer, p. 1–44, https://doi.org/10.1007/978-981-13-1666-1_1.

Burda, J., Gawęda, A., and Klötzli, U., 2011, Magma hybridization in the Western Tatra Mountains granitoid intrusion (S-Poland, Western Carpathians): Mineralogy and Petrology, v. 103, p. 19–36, https://doi.org/10.1007/s00710-011-0150-1.

Burke, K., Kidd, W.S.F., and Kusky, T., 1985, Is the Ventersdorp rift system of southern Africa related to a continental collision between the Kaapvaal and Zimbabwe cratons at 2. 64 Ga ago?: Tectonophysics, v. 115, p. 1–24, https://doi.org/10.1016/0040-1951(85)90096-4.

Chunnett, I.E., 1994, The Ventersdorp Contact Reef—A historical perspective: South African Journal of Geology, v. 97, p. 239–246.

Clendenin, C.W., Charlesworth, E.G., and Maske, S., 1988, An early Proterozoic three-stage rift system, Kaapvaal Craton, South Africa: Tectonophysics, v. 145, p. 73–86, https://doi.org/10.1016/0040-1951(88)90317-4.

Coetzee, F., 1988, Geological series [South Africa] 2830 Dundee: Geological Survey of South Africa, Pretoria, scale 1:250,000, 1 sheet.

Cole, E.G., 1994, Lithostratigraphy and depositional environment of the Archaean Nsuze Group, Pongola Supergroup [Ph.D. thesis]: Johannesburg, Rand Afrikaans University, 277 p.

Condie, K.C., 2003, Incompatible element ratios in oceanic basalts and komatiites: Tracking deep mantle sources and continental growth rates with time: Geochemistry Geophysics Geosystems, v. 4, p. 1–28, https://doi.org/10.1029/2002GC000333.

Cornell, D.H., Meintjes, P.G., van der Westhuizen, W.A., and Frei, D., 2017, Microbeam U-Pb Zircon dating of the Makwassie Formation and underlying units in the Ventersdorp Supergroup of South Africa: South African Journal of Geology, v. 120, p. 525–540, https://doi.org/10.25131/gssajg.120.4.525.

Cornell, D.H., Minnaar, H., Frei, D., and Kristoffersen, M., 2018, Precise microbeam dating defines three Archaean granitoid suites at the southwestern margin of the Kaapvaal Craton: Precambrian Research, v. 304, p. 21–38, https://doi.org/10.1016/j.precamres.2017.10.021.

Crow, C., and Condie, K.C., 1988, Geochemistry and origin of late Archean volcanics from the Ventersdorp Supergroup, South Africa: Precambrian Research, v. 42, p. 19–37, https://doi.org/10.1016/0301-9268(88)90008-3.

de Kock, M.O., Evans, D.A.D., and Beukes, N.J., 2009, Validating the existence of Vaalbara in the Neoarchean: Precambrian Research, v. 174, p. 145–154, https://doi.org/10.1016/j.precamres.2009.07.002.

de Kock, M.O., Beukes, N.J., and Armstrong, R.A., 2012, New SHRIMP U–Pb zircon ages from the Hartswater Group, South Africa: Implications for correlations of the Neoarchean Ventersdorp Supergroup on the Kaapvaal craton and with the Fortescue Group on the Pilbara craton: Precambrian Research, v. 204–205, p. 66–74, https://doi.org/10.1016/j.precamres.2012.02.007.

de Kock, M.O., Gumsley, A.P., Klausen, M.B., Söderlund, U., and Djeutchou, C., 2019, The Precambrian mafic magmatic record, including large igneous provinces of the Kalahari craton and its constituents: A paleogeographic review, *in* Srivastava, R.K., Ernst, R.E., and Peng, P., eds., Dyke Swarms of the World—A Modern Perspective: Amsterdam, Springer, p. 155–214, https://doi.org/10.1007/978-981-13-1666-1_5.

Denyszyn, S.W., Feinberg, J.M., Renne, P.R., and Scott, G.R., 2013, Revisiting the age and paleomagnetism of the Modipe Gabbro of South Africa: Precambrian Research, v. 238, p. 176–185, https://doi.org/10.1016/j.precamres.2013.10.002.

Duncan, R.A., Hooper, P.R., Rehacek, J., Marsh, J.S., and Duncan, A.R., 1997, The timing and duration of the Karoo igneous event, southern Gondwana: Journal of Geophysical Research: Solid Earth, v. 102, p. 18127–18138, https://doi.org/10.1029/97JB00972.

England, G.L., Rasmussen, B., McNaughton, N.J., Fletcher, I.R., Groves, D.I., and Krapez, B., 2001, SHRIMP

U–Pb ages of diagenetic and hydrothermal xenotime from the Archaean Witwatersrand Supergroup of South Africa: Terra Nova, v. 13, p. 360–367, https://doi.org/10.1046/j.1365-3121.2001.00363.x.

Ernst, R.E., 2014, Large Igneous Provinces: Cambridge, Cambridge University Press, 641 p., https://doi.org/10.1017/CBO9781139025300.

Ernst, R.E., and Buchan, K.L., 2001, Large mafic magmatic events through time and links to mantle-plume heads, *in* Ernst, R.E., and Buchan, K.L., eds., Mantle Plumes: Their Identification Through Time: Geological Society of America Special Paper 352, p. 483–575.

Ernst, R.E., and Youbi, N., 2017, How Large Igneous Provinces affect global climate, sometimes cause mass extinctions, and represent natural markers in the geological record: Palaeogeography, Palaeoclimatology, Palaeoecology, v. 478, p. 30–52, https://doi.org/10.1016/j.palaeo.2017.03.014.

Evans, D.A.D., Smirnov, A.V., and Gumsley, A.P., 2017, Paleomagnetism and U-Pb geochronology of the Black Range dykes, Pilbara Craton, Western Australia: A Neoarchean crossing of the polar circle: Australian Journal of Earth Sciences, v. 64, p. 225–237, https://doi.org/10.1080/08120099.2017.1289981.

Eriksson, P.G., Condie, K.C., van der Westhuizen, W., van der Merwe, R., de Bruiyn, H., Nelson, D.R., Altermann, W., Catuneanu, O., Bumby, A.J., Lindsay, J., and Cunningham, M.J., 2002, Late Archaean superplume events: A Kaapvaal–Pilbara perspective: Journal of Geodynamics, v. 34, p. 207–247, https://doi.org/10.1016/S0264-3707(02)00022-4.

Grobler, D.F., and Walraven, F., 1993, Geochronology of Gaborone Granite Complex extensions in the area north of Mafikeng, South Africa: Chemical Geology, v. 105, p. 319–337, https://doi.org/10.1016/0009-2541(93)90134-5.

Gumsley, A.P., de Kock, M.O., Rajesh, H.M., Knoper, M.W., Söderlund, U., and Ernst, R.E., 2013, The Hlagothi Complex: The identification of fragments from a Mesoarchaean large igneous province on the Kaapvaal Craton: Lithos, v. 174, p. 333–348, https://doi.org/10.1016/j.lithos.2012.06.007.

Gumsley, A., Olsson, J., Söderlund, U., de Kock, M., Hofmann, A., and Klausen, M., 2015, Precise U-Pb baddeleyite age dating of the Usushwana Complex, southern Africa—Implications for the Mesoarchaean magmatic and sedimentological evolution of the Pongola Supergroup, Kaapvaal Craton: Precambrian Research, v. 267, p. 174–185, https://doi.org/10.1016/j.precamres.2015.06.010.

Gumsley, A., Rådman, J., Söderlund, U., and Klausen, M., 2016, U-Pb baddeleyite geochronology and geochemistry of the White Mfolozi Dyke Swarm: Unravelling the complexities of 2.70–2.66 Ga dyke swarms across the eastern Kaapvaal Craton, South Africa: GFF, v. 138, p. 115–132, https://doi.org/10.1080/11035897.2015.1122665.

Gumsley, A.P., Chamberlain, K.R., Bleeker, W., Söderlund, U., de Kock, M.O., Larsson, E.R., and Bekker, A., 2017, Timing and tempo of the Great Oxidation Event: Proceedings of the National Academy of Sciences of the United States of America, v. 114, p. 1811–1816, https://doi.org/10.1073/pnas.1608824114.

Hammerbeck, E.C.I., 1982, The geology of the Usushwana Complex and associated formations—south-eastern Transvaal. Geological Survey of South Africa Memoir 70: Pretoria, Geological Survey of South Africa, 119 p.

Hatton, C.J., 1995, Mantle plume origin for the Bushveld and Ventersdorp magmatic provinces: Journal of African Earth Sciences, v. 21, p. 571–577, https://doi.org/10.1016/0899-5362(95)00106-9.

Heaman, L.M., 2009, The application of U-Pb geochronology to mafic, ultramafic and alkaline rocks: An evaluation of three mineral standards: Chemical Geology, v. 261, p. 43–52, https://doi.org/10.1016/j.chemgeo.2008.10.021.

Hiess, J., Condon, D.J., McLean, N., and Noble, S.R., 2012, $^{238}U/^{235}U$ Systematics in terrestrial uranium-bearing minerals: Science, v. 335, p. 1610–1614, https://doi.org/10.1126/science.1215507.

Hofmann, A., Kröner, A., Xie, H., Hegner, E., Belyanin, G., Kramers, J.D., Bolhar, R., Slabunov, A., Reinhardt, J., and Horváth, P., 2015, The Nhlangano gneiss dome in south-west Swaziland—A record of crustal destabilization of the eastern Kaapvaal craton in the Neoarchaean: Precambrian Research, v. 258, p. 109–132, https://doi.org/10.1016/j.precamres.2014.12.008.

Humbert, F., de Kock, M., Altermann, W., Elburg, M.A., Lenhardt, N., and Smith, A.J.B., 2018, Petrology, physical volcanology and geochemistry of a Paleoproterozoic large igneous province: The Hekpoort Formation in the southern Transvaal sub-basin (Kaapvaal Craton): Precambrian Research, v. 315, p. 232–256, https://doi.org/10.1016/j.precamres.2018.07.022.

Humbert, F., de Kock, M.O., Altermann, W., and Lenhardt, N., 2019, Neoarchean to early Paleoproterozoic within-plate volcanism of the Kaapvaal Craton: Comparing the Ventersdorp Supergroup and the Ongeluk and Hekpoort formations (Transvaal Supergroup), *in* Kröner, A. and Hofmann, A., eds., The Archaean Geology of the Kaapvaal Craton, Southern Africa: Amsterdam, Springer, p. 277–372, https://doi.org/10.1007/978-3-319-78652-0_11.

Irvine, T.N., and Baragar, W.R., 1971, A guide to the chemical classification of the common volcanic rocks: Canadian Journal of Earth Sciences, v. 8, p. 523–548, https://doi.org/10.1139/e71-055.

Jaffey, A.H., Flynn, K.F., Glendenin, L.E., Bentley, W.C., and Essling, A.M., 1971, Precision measurement of half-lives and specific activities of ^{235}U and ^{238}U: Physical Review C, v. 4, p. 1889–1906, https://doi.org/10.1103/PhysRevC.4.1889.

Janoušek, V., Farrow, C.M., and Erban, V., 2006, Interpretation of whole-rock geochemical data in igneous geochemistry: Introducing Geochemical Data Toolkit (GCDkit): Journal of Petrology, v. 47, p. 1255–1259, https://doi.org/10.1093/petrology/egl013.

Jones, C.R., and Hepworth, J.V., 1973, Geological map of Botswana: Geological Survey of Botswana, Gabarone, scale 1:1,000,000, 1 sheet.

Keyser, N., 1997, Geological map of the Republic of South Africa and the Kingdoms of Lesotho and Swaziland: Geological Survey of South Africa, Pretoria, scale 1:1,000,000, 1 sheet.

Klausen, M.B., Söderlund, U., Olsson, J.R., Ernst, R.E., Armoogan, M., Mkhize, S.W., and Petzer, G., 2010, Petrological discrimination among Precambrian dyke swarms: Eastern Kaapvaal craton (South Africa): Precambrian Research, v. 183, p. 501–522, https://doi.org/10.1016/j.precamres.2010.01.013.

Kositcin, N., McNaughton, N.J., Griffin, B.J., Fletcher, I.R., Groves, D.I., and Rasmussen, B., 2003, Textural and geochemical discrimination between xenotime of different origin in the Archaean Witwatersrand Basin, South Africa: Geochimica et Cosmochimica Acta, v. 67, p. 709–731, https://doi.org/10.1016/S0016-7037(02)01169-9.

Lubnina, N., Ernst, R., Klausen, M., and Söderlund, U., 2010, Paleomagnetic study of NeoArchean-Paleoproterozoic dykes in the Kaapvaal Craton: Precambrian Research, v. 183, p. 523–552, https://doi.org/10.1016/j.precamres.2010.05.005.

Ludwig, K.R., 2003, User's Manual for Isoplot 3.00—A Geochronological Toolkit for Microsoft Excel: Berkeley, Berkeley Geochronological Center, 74 p.

Ludwig, K.R., 2012, User's Manual for Isoplot 3.75: Berkeley, Berkeley Geochronology Center, 72 p.

Mapeo, R.B.M., Armstrong, R.A., Kampunzu, A.B., and Ramokate, L.V., 2004, SHRIMP U-Pb zircon ages of granitoids from the Western Domain of the Kaapvaal Craton, Southeastern Botswana: Implications for crustal evolution: South African Journal of Geology, v. 107, p. 159–172, https://doi.org/10.2113/107.1-2.159.

Marsh, J.S., Bowen, M.P., Rogers, N.W., and Bowen, T.B., 1992, Petrogenesis of late Archaean flood-type basic lavas from the Klipriviersberg Group, Ventersdorp Supergroup, South Africa: Journal of Petrology, v. 33, p. 817–847, https://doi.org/10.1093/petrology/33.4.817.

McDonough, W.F., and Sun, S.-S., 1995, The composition of the Earth: Chemical Geology, v. 120, p. 223–253, https://doi.org/10.1016/0009-2541(94)00140-4.

Meier, D.L., Heinrich, C.A., and Watts, M.A., 2009, Mafic dikes displacing Witwatersrand gold reefs: Evidence against metamorphic-hydrothermal ore formation: Geology, v. 37, p. 607–610, https://doi.org/10.1130/G25657A.1.

Meintjes, P.G., and van der Westhuizen, W.A., 2018a, Borehole LLE1—An intra-caldera succession of the Goedgenoeg and Makwassie Formations, Ventersdorp Supergroup: South African Journal of Geology, v. 121, p. 363–382, https://doi.org/10.25131/sajg.121.0034.

Meintjes, P.G., and van der Westhuizen, W.A., 2018b, Stratigraphy and geochemistry of the Goedgenoeg and Makwassie Formations, Ventersdorp Supergroup, in the Bothaville area of South Africa: South African Journal of Geology, v. 121, p. 339–362, https://doi.org/10.25131/sajg.121.0021.

Moore, M., Davis, D.W., Robb, L.J., Jackson, M.C., and Grobler, D.F., 1993, Archean rapakivi granite-anorthosite-rhyolite complex in the Witwatersrand basin hinterland, southern Africa: Geology, v. 21, p. 1031–1034, https://doi.org/10.1130/0091-7613(1993)021<1031:ARGARC>2.3.CO;2.

Nelson, D.R., Trendall, A.F., de Laeter, J.R., Grobler, N.J., and Fletcher, I.R., 1992, A comparative study of the geochemical and isotopic systematics of late Archaean flood basalts from the Pilbara and Kaapvaal Cratons: Precambrian Research, v. 54, p. 231–256, https://doi.org/10.1016/0301-9268(92)90072-V.

Olsson, J.R., Söderlund, U., Klausen, M.B., and Ernst, R.E., 2010, U-Pb baddeleyite ages linking major Archean dyke swarms to volcanic-rift forming events in the Kaapvaal craton (South Africa), and a precise age for the Bushveld Complex: Precambrian Research, v. 183, p. 490–500, https://doi.org/10.1016/j.precamres.2010.07.009.

Olsson, J.R., Söderlund, U., Hamilton, M.A., Klausen, M.B., and Helffrich, G.R., 2011, A late Archaean radiating dyke swarm as possible clue to the origin of the Bushveld Complex: Nature Geoscience, v. 4, p. 865–869, https://doi.org/10.1038/ngeo1308.

O'Neill, H.S.C., and Jenner, F.E., 2016, Causes of the compositional variability among the Ocean Floor Basalts: Journal of Petrology, v. 57, p. 2163–2194, https://doi.org/10.1093/petrology/egx001.

Paton, C., Woodhead, J.D., Hellstrom, J.C., Hergt, J.M., Greig, A., and Maas, R., 2010, Improved laser ablation U-Pb zircon geochronology through robust downhole fractionation correction: Geochemistry Geophysics Geosystems, v. 11, p. 1–36, https://doi.org/10.1029/2009GC002618.

Paton, C., Hellstrom, J., Paul, B., Woodhead, J., and Hergt, J., 2011, Iolite: Freeware for the visualisation and processing of mass spectrometric data: Journal of Analytical Atomic Spectrometry, v. 26, p. 2508–2518, https://doi.org/10.1039/c1ja10172b.

Pearce, J.A., 1996, A user's guide to basalt discrimination diagrams, *in* Wyman, D.A., ed., Trace Element Geochemistry of Volcanic Rocks: Applications for Massive Sulphide Exploration: Ottawa, Geological Association of Canada, p. 79–113.

Pearce, J.A., 2008, Geochemical fingerprinting of oceanic basalts with applications to ophiolite classification and the search for Archean oceanic crust: Lithos, v. 100, p. 14–48, https://doi.org/10.1016/j.lithos.2007.06.016.

Pelletier, R.A., 1937, Contributions to the geology of the far West Rand: South African Journal of Geology, v. 41, p. 127–162.

Petrus, J.A., and Kamber, B.S., 2012, VizualAge: A novel approach to laser ablation ICP-MS U-Pb geochronology data reduction: Geostandards and Geoanalytical Research, v. 36, p. 247–270, https://doi.org/10.1111/j.1751-908X.2012.00158.x.

Poujol, M., Kiefer, R., Robb, L.J., Anhaeusser, C.R., and Armstrong, R.A., 2005, New U-Pb data on zircons from the Amalia greenstone belt Southern Africa: Insights into the Neoarchaean evolution of the Kaapvaal Craton: South African Journal of Geology, v. 108, p. 317–332, https://doi.org/10.2113/108.3.317.

Reinhardt, J., Elburg, M.A., and Andersen, T., 2015, Zircon U-Pb age data and Hf isotopic signature of Kaapvaal basement granitoids from the Archaean White Mfolozi Inlier, northern Kwazulu-Natal: South African Journal of Geology, v. 118, p. 473–488, https://doi.org/10.2113/gssajg.118.4.473.

Söderlund, U., and Johansson, L., 2002, A simple way to extract baddeleyite (ZrO_2): Geochemistry: Geochemistry, Geophysics, Geosystems, v. 3, p. 1–7.

South African Committee for Stratigraphy (SACS), 1980, Stratigraphy of South Africa: Part 1, Lithostratigraphy of the Republic of South Africa, South West Africa/Namibia, and the Republics of Bophuthatswana, Transkei and Venda: Pretoria, Geological Survey of South Africa Handbook, 690 p.

Stacey, J.S., and Kramers, J.D., 1975, Approximation of terrestrial lead isotope evolution by a two-stage model: Earth and Planetary Science Letters, v. 26, p. 207–221, https://doi.org/10.1016/0012-821X(75)90088-6.

Stanistreet, I.G., and McCarthy, T.S., 1991, Changing tectono-sedimentary scenarios relevant to the development of the Late Archaean Witwatersrand Basin: Journal of African Earth Sciences, v. 13, p. 65–81, https://doi.org/10.1016/0899-5362(91)90044-Y.

Tankard, A.J., Jackson, M.P.A., Eriksson, K.A., Hobday, D.K., Hunter, D.R., and Minter, W.E.L., 1982, Crustal evolution of Southern Africa: New York, Springer-Verlag, 523 p., https://doi.org/10.1007/978-1-4613-8147-1.

Taylor, J., Stevens, G., Armstrong, R., and Kisters, A.F.M., 2010, Granulite facies anatexis in the Ancient Gneiss Complex, Swaziland, at 2.73 Ga: Mid-crustal metamorphic evidence for mantle heating of the Kaapvaal craton during Ventersdorp magmatism: Precambrian Research, v. 177, p. 88–102, https://doi.org/10.1016/j.precamres.2009.11.005.

Tyler, N., 1979, Stratigraphy, geochemistry and correlation of the Ventersdorp Supergroup in the Derdepoort area, west-central Transvaal: Transactions of the Geological Society of South Africa, v. 82, p. 133–147.

van der Westhuizen, W.A., de Bruijn, H., and Meintjes, P.G., 1991, The Ventersdorp Supergroup: An overview: Journal of African Earth Sciences, v. 13, p. 83–105, https://doi.org/10.1016/0899-5362(91)90045-Z.

van der Westhuizen, W.A., de Bruijn, H., and Meintjes, P.G., 2006, The Ventersdorp Supergroup, *in* Jonson, M.R., Anhaeusser, C.R., and Thomas, R.J., eds., Geology of South Africa: Johannesburg/Pretoria, Geological Society of South Africa/Council for Geoscience, p. 187–208.

Visser, J.N.J., and Grobler, N.J., 1985, Syndepositional volcanism in the Rietgat and arenaceous Bothaville Formations, Ventersdorp Supergroup (late Archaean-early Proterozoic), in South Africa: Precambrian Research, v. 30, p. 153–174, https://doi.org/10.1016/0301-9268(85)90049-X.

Walraven, F., 1986, Geological series [South Africa] 2630 Mbabane: Geological Survey of South Africa, Pretoria, scale 1:250,000, 1 sheet.

Walraven, F., Grobler, D.F., and Key, R.M., 1996, Age equivalence of the Plantation Porphyry and the Kanye Volcanic Formation, southeastern Botswana: South African Journal of Geology, v. 99, p. 23–31.

Walraven, F., Smith, C.B., and Kruger, F.J., 1991, Age determinations of the Zoetlief Group—A Ventersdorp Supergroup correlative: South African Journal of Geology, v. 94, p. 220–227.

Wiles, J.W., 1971, Provisional geological map of Rhodesia: Geological Survey of Rhodesia, Salisbury, scale 1:1,000,000, 1 sheet.

Winchester, J.A., and Floyd, P.A., 1977, Geochemical discrimination of different magma series and their differentiation products using immobile elements: Chemical Geology, v. 20, p. 325–343, https://doi.org/10.1016/0009-2541(77)90057-2.

Wingate, M.T.D., 1998, A palaeomagnetic test of the Kaapvaal-Pilbara (Vaalbara) connection at 2.78 Ga: South African Journal of Geology, v. 101, p. 257–274.

Winter, H. de la R., 1976, A lithostratigraphic classification of the Ventersdorp succession: Transactions of the Geological Society of South Africa, v. 79, p. 31–48.

Zeh, A., Ovtcharova, M., Wilson, A.H., and Schaltegger, U., 2015, The Bushveld Complex was emplaced and cooled in less than one million years—Results of zirconology, and geotectonic implications: Earth and Planetary Science Letters, v. 418, p. 103–114, https://doi.org/10.1016/j.epsl.2015.02.035.

Science Editor: Rob Strachan

Manuscript Received 14 January 2019
Revised Manuscript Received 22 September 2019
Manuscript Accepted 8 November 2019

Printed in the USA